OTREC

FINAL REPORT

Analyzing and Quantifying the Impact of Congestion on LTL Industry Costs and Performance in the Portland Metropolitan Region

OTREC-RR-12-10
July 2012

ANALYZING AND QUANTIFYING THE IMPACT OF CONGESTION ON LTL INDUSTRY COSTS AND CO$_2$ EMISSIONS IN THE PORTLAND METROPOLITAN REGION

Final Report

OTREC-RR-12-10

by

Miguel Figliozzi, Ph.D.

Portland State University

for

OREGON TRANSPORTATION RESEARCH
AND EDUCATION CONSORTIUM

P.O. Box 751
Portland, OR 97207

July 2012

Technical Report Documentation Page

1. Report No. OTREC-RR-12-10	2. Government Accession No.	3. Recipient's Catalog No.
4. Title and Subtitle Analyzing and Quantifying the Impact of Congestion on LTL Industry Costs and Performance in the Portland Metropolitan Region		5. Report Date
		6. Performing Organization Code
7. Author(s) Miguel Figliozzi Portland State University Civil and Environmental Engineering P.O. Box 751 Portland, OR, 97207		8. Performing Organization Report No.
9. Performing Organization Name and Address		10. Work Unit No. (TRAIS)
		11. Contract or Grant No. 2009-276
12. Sponsoring Agency Name and Address Oregon Transportation Research and Education Consortium (OTREC) P.O. Box 751 Portland, Oregon 97207		13. Type of Report and Period Covered
		14. Sponsoring Agency Code
15. Supplementary Notes		

16. Abstract

Increased congestion during peak morning and afternoon periods in urban areas is increasing logistics costs. In addition, environmental, social, and political pressures to limit the impacts associated with CO_2 emissions are mounting rapidly. A key challenge for transportation agencies and businesses is to improve the efficiency of urban freight and commercial vehicle movements while ensuring environmental quality, livable communities, and economic growth. However, research and policy efforts to analyze and quantify the impacts of congestion and freight public policies on carriers operations and CO_2 emissions are hindered by the complexities of vehicle routing problems with time-dependent travel times and the lack of network-wide congestion data. This research focuses on the analysis of costs and CO_2 emissions for different levels of congestion and time-definitive customer demands. Travel time data from an extensive archive of freeway sensors, time-dependent vehicle routing algorithms, and problems-instances with different types of binding constraints are used to analyze the impacts of congestion on commercial vehicle emissions.

17. Key Words
Urban Freight, Congestion Impacts, Vehicle Routing, Greenhouse gas emissions
		18. Distribution Statement
		   No restrictions. Copies available from OTREC:
		   www.otrec.us	

19. Security Classification (of this report) Unclassified	20. Security Classification (of this page) Unclassified	21. No. of Pages 66	22. Price

ACKNOWLEDGEMENTS

DISCLAIMER

TABLE OF CONTENTS

LIST OF TABLES

LIST OF FIGURES

EXECUTIVE SUMMARY

Urban congestion presents considerable challenges to time-definite transportation service providers. Package, courier, and less-than-truckload (LTL) operations and costs are severely affected by increasing congestion levels. With congestion increasing at peak-hour morning and afternoon periods, public policies and logistics strategies that avoid or minimize deliveries during congested periods have become crucial for many operators and public agencies. However, in many cases these strategies or policies can introduce unintended side effects such as higher labor costs, shorter working hours, and tighter customer time windows. Research efforts to analyze and quantify the impacts of congestion on costs and CO_2 emissions are hindered by the complexities of vehicle routing problems with time-dependent travel times and the lack of network-wide congestion data. This research utilizes: (a) real-world road network data to estimate travel distance and time matrices, (b) land use and customer data to localize and characterize demand patterns, (c) congestion data from an extensive archive of freeway and arterial street traffic sensor data to estimate time-dependent travel times, and (d) an efficient time-dependent vehicle routing (TDVRP) solution method to design routes.

Novel solutions approaches and algorithms are developed to (a) integrate real-world road network and travel data to TDVRP solution methods and (b) quantify the impact of congestion on LTL emissions. The results show the dramatic impact of congestion on carriers' fleet sizes and distance travelled; the impacts of congestion tend to be higher for depots located in suburban areas and downtown customer service areas. Results also indicate that the impacts of congestion or speed limits on commercial vehicle emissions are significant, but are difficult to predict since it is shown that it is possible to have instances where total route distance or duration increases but emissions decrease. Public agencies should carefully study the implications of policies that regulate depot locations and travel speeds as they may have unintended negative consequences in terms of CO_2 emissions.

1.0   INTRODUCTION

1.1   BACKGROUND

Congested urban areas present considerable challenges for LTL (less-than-truckload) carriers, courier services and industries that require frequent and time-sensitive deliveries. With congestion increasing at peak-hour morning and afternoon periods, public policies and logistics strategies that avoid or minimize deliveries during congested periods have become crucial for many operators and public agencies. However, in many cases, these strategies and policies can introduce unintended side effects such as higher labor costs, shorter working hours and tighter customer time windows.

While current research on vehicle routing, with an emphasis on algorithms, is extensive, much less attention has been devoted to investigating the impacts of congestion on carrier operations. Furthermore, most algorithms to solve the time-dependent vehicle routing problem (TDVRP) found in the existing literature do not deal with the estimation of real-world distance and time-dependent travel time matrices.

Urban freight is also responsible for a large share, or in some cities the largest share, of unhealthy air pollution in terms of sulphur oxide, particulate matter, and nitrogen oxides in urban areas such as London, Prague and Tokyo (OECD, 2003; Crainic et al., 2009). The fast rate of commercial vehicle activity growth over recent years and the higher impact of commercial vehicles (when compared to passenger vehicles) are increasing preexisting concerns over their cumulative effect in urban areas. In particular, environmental, social and political pressures to limit the impacts associated with carbon dioxide (CO_2) emissions and fossil fuel dependence are mounting rapidly.

A key challenge for transportation agencies is to improve the efficiency of urban freight and commercial vehicle movements while ensuring environmental quality, livable communities and economic growth. Research in the area of city logistics has long recognized the need for a balanced approach to reduce shippers' and carriers' logistics costs as well as the community's traffic congestion and environmental problems (Taniguchi et al., 2003; Crainic et al., 2004).

Although past and current research efforts into vehicle routing algorithms and scheduling are extensive (Cordeau et al., 2006) most research efforts have ignored freight-related environmental and social externalities. Furthermore, the body of research devoted to investigating the impacts of congestion on urban commercial vehicle operations and time-dependent travel times is relatively scant. In the existing literature, there are no published congestion case studies involving CO_2 emission levels, time-dependent vehicle routing problems, and a diverse set of customer constraints.

1.2   RESEARCH GOALS AND REPORT ORGANIZATION

This research analyzes the impacts of congestion on LTL carriers operations and emissions. Two different questions are answered:

(1) What are the impacts of congestion on LTL carriers' greenhouse gas emissions? What are the impacts of customer- depot locations on total greenhouse gas emissions?

(2) How can we integrate real-world road network and travel data into our analysis? How can we use existing loop detector data to improve congestion analysis?

This report is organized as follows: Section 2 provides a brief literature review. Section 3 presents the mathematical formulation of the time-dependent, hard time windows routing problem as well as an expression to calculate CO_2 emissions. Section 4 describes the Portland LTL emissions case study, its data sources and the solution approach. Section 5 presents and analyzes CO_2 emissions experimental results. Section 6 presents the methodology to incorporate real-world travel and congestion data. Section 7 describes the Portland case study. Section 8 analyzes experimental results utilizing the methodology presented in Section 6 and the Section 7 case study.

2.0   LITERATURE REVIEW

The literature review for this report covers three main areas of research: (a) the effects of congestion and travel time variability on vehicle tours and logistics; (b) the impact of travel speeds on commercial vehicle emissions; and (c) time-dependent vehicle routing problems.

Direct and indirect costs of congestion on passenger travel time, shipper travel time and market access, production and labor productivity have been widely studied and reported in the available literature. The work of Weisbrod et al. (2001) provides a broad review of this literature. Survey results suggest that the type of freight operation has a significant influence on how congestion affects carriers' operations and costs. For example, results from a California survey indicate that congestion is perceived as a serious problem for companies specializing in less-than-truckload (LTL), refrigerated and intermodal cargo (Golob and Regan, 2001). These results largely agree with reports analyzing the effects of traffic congestion in the Portland region (ERDG, 2005, 2007).

Congestion has a significant impact on routes where delivery times are heavily restricted by customer time windows and schedules. In addition, there may be a fairly inelastic relationship between delivery costs and customer's demand characteristics and levels. For example, Holguin-Veras et al. (2006) investigated the effects of New York City's congestion pricing on LTL deliveries and found little changes because delivery times were determined by customer time windows and schedules. Figliozzi (2007, 2009a) analyzes the effects of congestion on vehicle tour characteristics using continuous approximations to routing problems. Figliozzi (2007) analyzes how constraints and customer service time affect trip generation using a tour classification based on supply chain characteristics and route constraints. This work also reveals that changes in both vehicle kilometers traveled (VKT) and vehicle hours traveled (VHT) differ by type of tour and routing constraint. Hard time windows are the type of constraint that most severely increases VKT and VHT. Figliozzi (2009a) models the effects of congestion and travel time variability on vehicle tour characteristics; analytical and numerical results indicate that travel speed reductions and depot-customer travel distances are the key factors that exacerbate the impacts of travel time variability. Quak and Koster (2009) utilized a fractional factorial design and regression analysis to quantify the impacts of delivery constraints and urban freight policies. Quak and Koster (2009) findings confirm previous results. Vehicle restrictions that affected customers with time window constraints did not have an impact on customer costs. However, vehicle restrictions are found to be costly when vehicle capacity is limited.

There is extensive literature related to vehicle emissions, and several laboratory and field methods are available to estimate vehicle emissions rates (Ropkins et al., 2009). Research results indicate that CO_2 is the predominant transportation greenhouse gas (GHG) and is emitted in direct proportion to fuel consumption, with a variation by type of fuel (ICF, 2006). For most vehicles, fuel consumption and the rate of CO_2 per mile traveled decreases as vehicle operating speed increases up to an optimal speed, and then begins to increase again (ICF, 2006). Furthermore, the relationship between emission rates and travel speed is not linear.

Congestion has a great impact on CO_2 vehicle emissions and fuel efficiency. In real driving conditions, there is a rapid non-linear growth in emissions and fuel consumption as travel speeds fall below 30 mph (Barth and Boriboonsomsin, 2008). CO_2 emissions double on a per mile basis when speed drops from 30 mph to 12.5 mph or when speed drops from 12.5 mph to 5 mph. These results were obtained using an emission model and freeway sensor data in California and weighted on the basis of a typical light-duty fleet mix in 2005. Frequent changes in speed (i.e., stop-and-go traffic conditions) increases emission rates because fuel consumption is a function of not only speed but also acceleration rates (Frey et al., 2008).

Some researchers have conducted surveys that indicate that substantial emission reductions can be obtained if companies improve the efficiency of routing operations (Léonardi and Baumgartner, 2004; Baumgartner et al., 2008). Other researchers using queuing theory (Woensel et al., 2001) modeled the impact of traffic congestion on emissions and recommend that private and public decision makers take into account the high impact of congestion on emissions. From an operational perspective, carriers cannot take into account the impact of congestion on emissions unless time-dependent travel times are considered when designing distribution or service routes. While classic versions of the VRP, specifically the capacitated VRP (CVRP), or VRP with time windows (VRPTW) have been widely studied in the available literature (Cordeau et al., 2006), while time-dependent problems have received considerably less attention. The Time Dependent Vehicle Routing Problem (TDVRP) takes into account that links in a network have different costs or speeds during the day. Typically, this time dependency is used to represent varying traffic conditions. The TDVRP was originally formulated by Malandraki and Daskin (1992). Time-dependent models are significantly more complex and computationally demanding than static VRP models. Approaches to solve the TDVRP can be found in the work of several authors (Malandraki, 1989; Ahn and Shin, 1991; Jung and Haghani, 2001; Ichoua et al., 2003; Fleischmann et al., 2004; Haghani and Jung, 2005; Donati et al., 2008; Figliozzi, 2009c). The reader is referred to Figliozzi (2009c) for an up-to-date and extensive TDVRP literature review and the description of benchmark problems.

TDVRP instances are considerably more demanding than static VRP instances in terms of data requirements and computational time. However, solving more realistic TDVRP instances may indirectly achieve environmental benefits in congested areas because total route durations and distances can be reduced even though emissions are not part of the objective function (Sbihi and Eglese, 2007). Though the emissions problem is complex, as shown in Section 5, it is possible to construct instances where distance or duration increases but emissions decrease. Palmer (2008) studied the minimization of CO_2 emissions utilizing real network data, multi-stop routes averaging almost 10 deliveries per route, and shortest paths of Surrey county in the U.K. However, Palmer's methodology does not allow for time-dependent speeds or multi-stop routes. Figliozzi (2010) formulated the emissions vehicle routing problem (EVRP) with time-dependent travel times, hard time windows and capacity constraints. In addition to the usual binary variables for assigning vehicles to customers, this is the first VRP with time-windows formulation to include speed and departure time as decision variables and also present conditions and algorithms

to determine efficient departure times and travel speeds. Figliozzi (2010) showed that a routing formulation and solution algorithm that takes into account congestion and aims to minimize CO_2 emissions can produce significant reductions in emission levels with relatively small increases in distance traveled or fleet size.

3.0 NOTATION AND PROBLEM FORMULATION

This section introduces the basic optimization problem that can be used to estimate emissions when LTL carriers optimize deliveries based on cost and service considerations. Unlike the formulation presented by Figliozzi (2010), in this research travel speeds are not optimized to reduce emissions, but are introduced as decision variables to represent restrictions due to freight policy measures, congestion or time windows. Hence, carriers in this research continue "business as usual" without internalizing the costs of emissions.

Using a traditional flow-arc formulation (Desrochers et al., 1988) and building upon a formulation of the TDVRP with time windows (Figliozzi, 2009b)b), the vehicle routing problem studied in this research can be described as follows. Let $G = (V, A)$ be a graph where $A = \{(v_i, v_j) : i \neq j \wedge i, j \in V\}$ is an arc set and the vertex set is $V = (v_0, \ldots, v_{n+1})$. Vertices v_0 and v_{n+1} denote the depot at which vehicles of capacity q_{max} are based. Each vertex in V has an associated demand $q_i \geq 0$, a service time $g_i \geq 0$, and a service time window $[e_i, l_i]$; in particular the depot has $g_0 = 0$ and $q_0 = 0$. The set of vertices $C = \{v_1, \ldots, v_n\}$ specifies a set of n customers. The arrival time of a vehicle at customer $i, i \in C$ is denoted a_i and its departure time b_i. Each arc (v_i, v_j) has an associated constant distance $d_{ij} \geq 0$ and a travel time $t_{ij}(b_i) \geq 0$ which is a function of the departure time from customer i. The set of available vehicles is denoted K. The cost per unit distance traveled is denoted c_d. A binary decision variable x_{ij}^k indicates whether vehicle k travels between customers i and j. A real decision variable y_i^k indicates service start time if customer i is served by vehicle k; hence the departure time is given by the customer service start time plus service time $b_i = y_i^k + g_i$.

In the capacitated vehicle routing problem with time windows (VRPTW) it is traditionally assumed that carriers minimize the number of vehicles as a primary objective and distance traveled as a secondary objective without violating time windows, route durations or capacity constraints. The problem analyzed in this research follows this traditional approach; however, CO_2 emissions are also computed to analyze emissions tradeoffs due to policy restrictions, time windows or congestion levels.

3.1 PROBLEM FORMULATION

The primary objective is fleet size minimization as defined by (1) and the secondary objective is the minimization of distance traveled and route duration costs.

PRIMARY OBJECTIVE

$$minimize \quad \sum_{k \in K} \sum_{j \in C} x_{0j}^k , \tag{1}$$

SECONDARY OBJECTIVE

$$minimize \quad c_d \sum_{k \in K} \sum_{(i,j) \in V} d_{ij} x_{ij}^k \tag{2}$$

CONSTRAINTS

$$\sum_{i \in C} q_i \sum_{j \in V} x_{ij}^k \leq q_{\max} , \quad \forall k \in K \tag{3}$$

$$\sum_{k \in K} \sum_{j \in V} x_{ij}^k = 1, \quad \forall i \in C \tag{4}$$

$$\sum_{i \in V} x_{il}^k - \sum_{i \in V} x_{lj}^k = 0 , \quad \forall l \in C, \forall k \in K \tag{5}$$

$$x_{i0}^k = 0, x_{n+1,i}^k = 0, \quad \forall i \in V, \forall k \in K \tag{6}$$

$$\sum_{j \in V} x_{0j}^k = 1, \quad \forall k \in K \tag{7}$$

$$\sum_{j \in V} x_{j,n+1}^k = 1, \quad \forall k \in K \tag{8}$$

$$e_i \sum_{j \in V} x_{ij}^k \leq y_i^k , \quad \forall i \in V, \forall k \in K \tag{9}$$

$$l_i \sum_{j \in V} x_{ij}^k \geq y_i^k , \quad \forall i \in V, \forall k \in K \tag{10}$$

$$x_{i,j}^k (y_i^k + g_i + t_{i,j}(y_i^k + g_i)) \leq y_j^k , \quad \forall (i,j) \in A, \forall k \in K \tag{11}$$

$$x_{ij}^k \in \{0,1\}, \quad \forall (i,j) \in A, \forall k \in K \tag{12}$$

$$y_i^k \in \Re , \quad \forall i \in V, \forall k \in K \tag{13}$$

The constraints are defined as follows: vehicle capacity cannot be exceeded (3); all customers must be served (4); if a vehicle arrives at a customer it must also depart from that customer (5); routes must start and end at the depot (6); each vehicle leaves from and returns to the depot

exactly once, (7) and (8) respectively; service times must satisfy time window start (9) and ending (10) times; and service start time must allow for travel time between customers (11). Decision variables type and domain are indicated in (12) and (13).

3.2 EMISSIONS MODELING

CO_2 emissions are proportional to the amount of fuel consumed, which is a function of travel speed and distance traveled, among other factors. In this research it is assumed that the weight of the products loaded does not significantly affect CO_2 emission levels in relation to the impacts of travel speeds. To incorporate recurrent congestion impacts and following a standard practice in TDVRP models, the depot working time $[e_0, l_0]$ is partitioned into M time periods $\mathbf{T} = T^1, T^1, ..., T^M$; each period T^m has an associated constant travel speed $0 \leq s^m$ in the time interval $T^m = [\underline{t}^m, \overline{t}^m]$.

For each departure time b_i and each pair of customers i and j, a vehicle travels a non-empty set of speed intervals $S_{ij}(b_i) = \{s_{ij}^m(b_i), s_{ij}^{m+1}(b_i), ..., s_{ij}^{m+p}(b_i)\}$ where $s_{ij}^m(b_i)$ denotes the speed at departure time, $s_{ij}^{m+p}(b_i)$ denotes the speed at arrival time, and $p+1$ is the number of time intervals utilized. The departure time at speed $s_{ij}^m(b_i)$ takes place in period T^m, the arrival time at speed $s_{ij}^m(b_i)$ takes place in period T^{m+p}, and $1 \leq m \leq m + p \leq M$.

For the sake of notational simplicity the departure time will be dropped even though speed intervals and distance intervals are a function of departure time b_i. The corresponding set of distances and times traveled in each time period are denoted $D_{ij}(b_i) = \{d_{ij}^m, d_{ij}^{m+1}, ..., d_{ij}^{m+p}\}$ and $T_{ij}(b_i) = \{t_{ij}^m, t_{ij}^{m+1}, ..., t_{ij}^{m+p}\}$ respectively.

For heavy duty vehicles, the Transport Research Laboratory has developed a function that links emissions, distance traveled, and travel speeds for heavy duty trucks (TRL, 1999):

$$[\alpha_0 + \alpha_1 s_{ij}^l + \alpha_2 (s_{ij}^l)^3 + \alpha_3 (\frac{1}{(s_{ij}^l)^2})] d_{ij}^l \qquad (14)$$

With the appropriate conversion factor, the output from (14) can be converted from CO_2 tons per unit of distance (kilometers or miles) to fuel efficiency (diesel consumed per kilometer or mile) since fuel consumption and CO_2 emissions are closely correlated (ICF, 2006). The coefficients $\{\alpha_0, \alpha_1, \alpha_2, \alpha_3\}$ = {1576.0; -17.6; 0.00117; 36067.0} are parameters for the heavy duty truck type. For other vehicle types (e.g., medium or light duty trucks) there may be other polynomial terms (TRL, 1999). These parameters are likely to change over time as technology and engines evolve; however, the CO_2 percentage changes and tradeoffs analysis presented in Section 5 are likely to

remain valid unless there are dramatic changes in the shape of the speed-emissions curve. The optimal travel speed that minimizes emissions per mile is assumed to be the speed $s*$, which for expression (14) the value is $s* \approx 44$ mph or 71 kmh. Expression (14) outputs CO_2 emissions in Kg/km when the speed is expressed in km/h. As congestion increases, the amount and cost of emissions increases dramatically. In addition, below free-flow travel speeds, real-world stop-and-go conditions further increase emissions (Barth and Boriboonsomsin, 2008). Figure 1 depicts the change in emissions between steady-state and real-world congested conditions. CO_2 emission rates under real-world congested conditions can be up to 40% higher than emission rates under steady-state conditions.
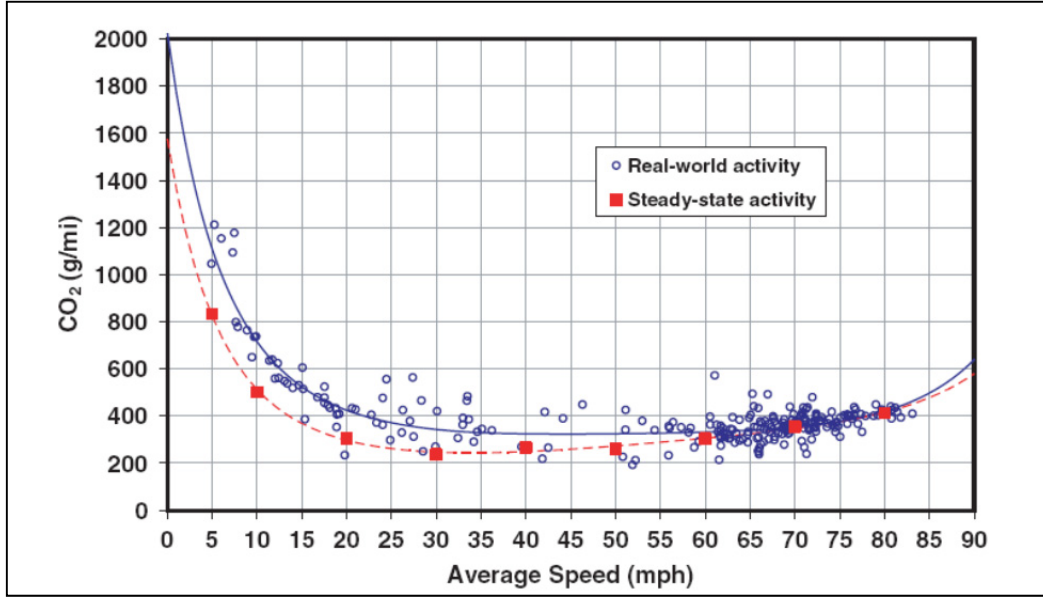
Figure 1. CO_2 emissions as a function of average speed (Barth and Boriboonsomsin, 2008)

The volume of emissions generated by travelling from customer i to customer j and departing at time b_i is denoted $v_{ij}(b_i)$:

$$v_{ij}(b_i) = \sum_{l=0}^{l=p} [\alpha_0(s_{ij}^l) + \alpha_1 s_{ij}^l + \alpha_2(s_{ij}^l)^3 + \alpha_3 \frac{1}{(s_{ij}^l)^2} d_{ij}^l] \tag{15}$$

Expression (15) provides a simple yet good approximation for real-world CO_2 emissions vs. travel speed profiles. Acceleration impacts are not considered because detailed speed profiles will be required; however, to account for the emission rate increases in stop-and-go traffic conditions, the term $\alpha_0(s_{ij}^l)$ could be adjusted.

3.3 SPEED CONSTRAINTS

Travel speeds are limited by speed limits or congestion. As indicated by constraint (16), a vehicle traveling between two customers i, j cannot exceed the travel speed for that link in period of time l.

$$\underline{s}_{ij}^{l} \leq s_{ij}^{l} \leq \overline{s}_{ij}^{l} \tag{16}$$

In addition, travel speeds are also limited by road characteristics. To represent different road characteristics between two customers i, j the segment of distance d_{ij} is partitioned into a set of $R(i, j)$ segments that for the partial distance set:

$$\{r_{ij}^{1}, r_{ij}^{2}, ..., r_{ij}^{R(i,j)}\} \text{ such that } d_{ij} = \sum_{l'=1}^{l'=R(i,j)} r_{ij}^{l'}$$

Each segment $r_{ij}^{l'}$ has an upper and lower speed bounds. Combining speed constraints due to time of the day and road section, we obtain the more general constraint expression (17) for time of day l and section l' between customers i, j:

$$\underline{s}_{ij}^{l,l'} \leq s_{ij}^{l,l'} \leq \overline{s}_{ij}^{l,l'} \tag{17}$$

13

4.0 PORTLAND EMISSIONS CASE STUDY

Considered a gateway to international sea and air freight transport, the city of Portland has established itself both in name and trade as an important component of both international and domestic freight movements. Its favorable geography to both international ocean and domestic river freight via the Columbia River is also complimented by its connection to Interstate 5 (I-5), providing good connectivity to southern California ports and international freight traffic from Mexico and Canada (EDRG, 2007). Recent increases in regional congestion, however, have hindered freight operations considerably and brought about a substantial increase in delivery costs (Conrad and Figliozzi, 2010).
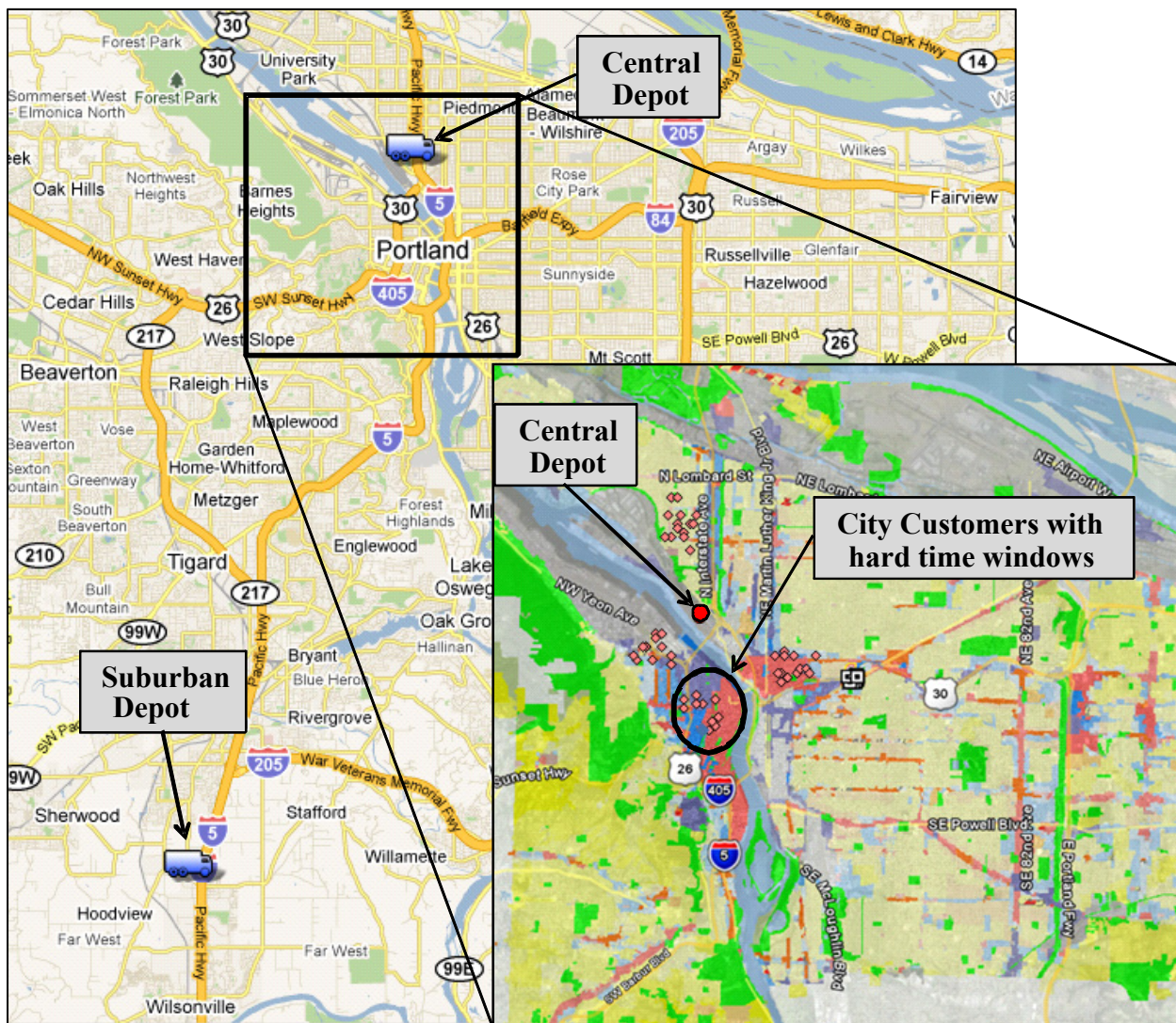
Figure 2. Depots and customer locations (base map sourced from Google Maps[1])

The I-5 freeway corridor provides the main north-south freight corridor and is used by most carriers delivering in downtown Portland, regional through traffic and many commuters. Land use patterns are used to locate two carrier's depots in warehousing/industrial areas that are located in relatively central and suburban locations, respectively. The I-5 freeway corridor, even under congested conditions, provides the shortest distance and time path between the urban and suburban depot and downtown Portland. Freeway, arterial and local segments are established for each path as required by expression (17).

Figure 2 also shows the relative location of downtown Portland, the I-5 corridor, the central depot, and the suburban depot. Experimental results described in Section 5 utilize the central and suburban depot locations shown in Figure 2 as well as an intermediate depot location (not shown in Figure 2) located between the central customers and the suburban depot. The intermediate depot is located on I-5 at a distance that is approximately one-third of the distance between the central customers and the suburban depot. The central, intermediate and suburban depots are located in areas with warehousing or related land uses or commercial activities.

4.1   TRAVEL SPEED DATA

Time-dependent travel speed data comes from 436 inductive loop detectors along interstate freeways in the Portland metropolitan area. Traffic data is systematically archived in the Portland Oregon Transportation Archived Listing (PORTAL). A complete description of this data source is given by Bertini et al. (2005). The travel speeds used in this research are calculated from 15-minute archived travel time data averaged over the year 2007 along the I-5 freeway corridor spanning from the Portland suburb of Wilsonville to Vancouver, WA. In addition, Portland State University had access to truck GPS location and time data that can be used to calculate travel speeds (Wheeler and Figliozzi, 2009). Figure 3 compares a typical week of average time-dependent travel time data using sensor data from PORTAL and GPS-based data for a section of I-5; historical travel time speeds based on sensor data are a good proxy for truck travel speeds.

Figure 3 also shows that free-flow travel speeds, around 60 miles per hour, take place at night – mostly between 9 p.m. and 6 a.m. Some commercial vehicles travel at speeds as high as 70 or 75 miles per hour. This research assumes that travel speeds between 6 a.m. and 9 p.m. are a function of time of day. The base scenario, uncongested travel times, assumes a constant time dependent speed of 65 miles per hour in the freeways and 30 miles per hour in the arterial network. Travel speed on arterials is based on speed limits during uncongested hours and estimating congested travel times based on patterns observed in the Portland area (Wolfe et al., 2007). The percentage of local street travel is relatively small and mostly limited to connections between customers and freeways/arterials. Local speed is assumed to have a constant value of 10 miles per hour.
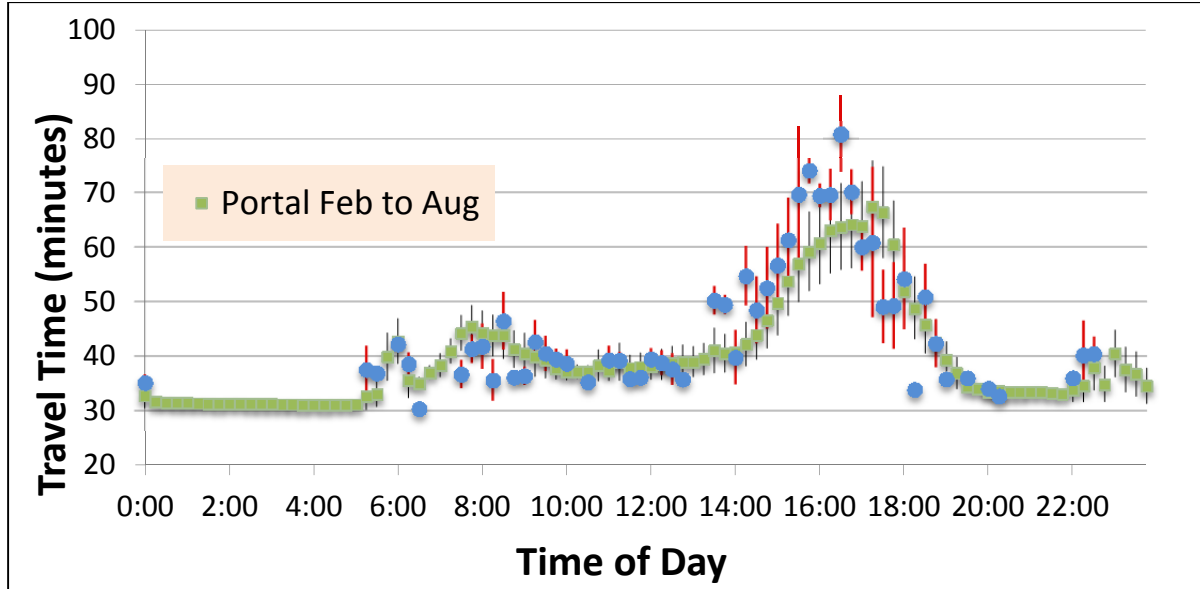
Figure 3: Example of travel speed variations using sensor and GPS data

4.2   CUSTOMER DATA

A primary goal of this research is to quantify the impact of congestion on emissions for typical customer constraints in the Portland metropolitan area. It is assumed that delivery hours correspond to normal business hours between 8 a.m. and 4 p.m. Since delivery times are heavily dictated by customer time windows and schedules (Holguin-Veras et al., 2006), it is assumed that vehicles depart from each depot so that they serve the first customer after 8 a.m.

The distribution of customers' requests is assumed to take place in downtown Portland, as shown in Figure 2. The literature indicates that congestion impacts on route characteristics are highly dependent on the type of binding constraint. To study a diverse set of binding constraints and customer distributions, the experimental design is based on the classical instances of the VRP with time windows proposed by Solomon (1987). The Solomon instances include distinct spatial customer distributions, vehicles' capacities, customer demands, and customer time windows. These problems have not only been widely studied in the operations research literature but the datasets are readily available.

The well-known 56 Solomon benchmark problems for vehicle routing problems with hard time windows are based on six groups of problem instances with 100 customers. The six problem classes are named C1, C2, R1, R2, RC1, and RC2. Customer locations were randomly generated (problem sets R1 and R2), clustered (problem sets C1 and C2), or mixed with randomly generated and clustered customer locations (problem sets RC1 and RC2). Problem sets R1, C1, and RC1 have a shorter scheduling horizon, tighter time windows, and fewer customers per route than problem sets R2, C2, and RC2, respectively. Demand constraints are binding for C1 and C2 problems whereas time-window constraints are binding for R1, R2, RC1, and RC2

17

problems. In this research, the Solomon customer time windows are made proportional to the assumed normal business hours between 8 a.m. and 4 p.m. so the original demand and time window constraints are maintained. Customer locations have been scaled to fit the downtown Portland area, but the relative spatial distribution among customers has been preserved.

4.3   SOLUTION ALGORITHM

The time-dependent vehicle routing problems are solved using the route construction and improvement algorithm described in detail in Figliozzi (2009c). This approach, also denoted IRCI for *Iterated Route Construction and Improvement*, has also been successfully applied to VRP problems with soft time windows (Figliozzi, 2009b). As in previous research efforts with a exploratory and policy motivation (Quak and de Koster, 2007), the focus of this research is not on finding optimal routes for simpler problems (i.e., constant travel time problems), but on approximating carriers' route planning as well as possible and capturing the tradeoff between congestion, depot locations, customer characteristics, and CO_2 emissions in the case study area.

The TDVRP solution algorithm consists of a route construction phase and a route improvement phase, each utilizing two separate algorithms (Figure 4). During route construction, the auxiliary routing algorithm H_r repeatedly determines feasible routes using a greedy insertion approach with the construction algorithm H_c assigning customers and sequencing the routes. Route improvement is done first with the route improvement algorithm H_i which compares similar routes and consolidates customers into a set of improved routes. Lastly, the service time improvement algorithm H_y eliminates any time window violations, and then reduces the route duration without introducing additional early or late time window violations. These tasks are accomplished by using the arrival time and departure time algorithms H_{yf} and H_{yb}, respectively, and re-sequencing customers as needed. It is with these algorithms that the travel time data are inserted into the solution algorithm.
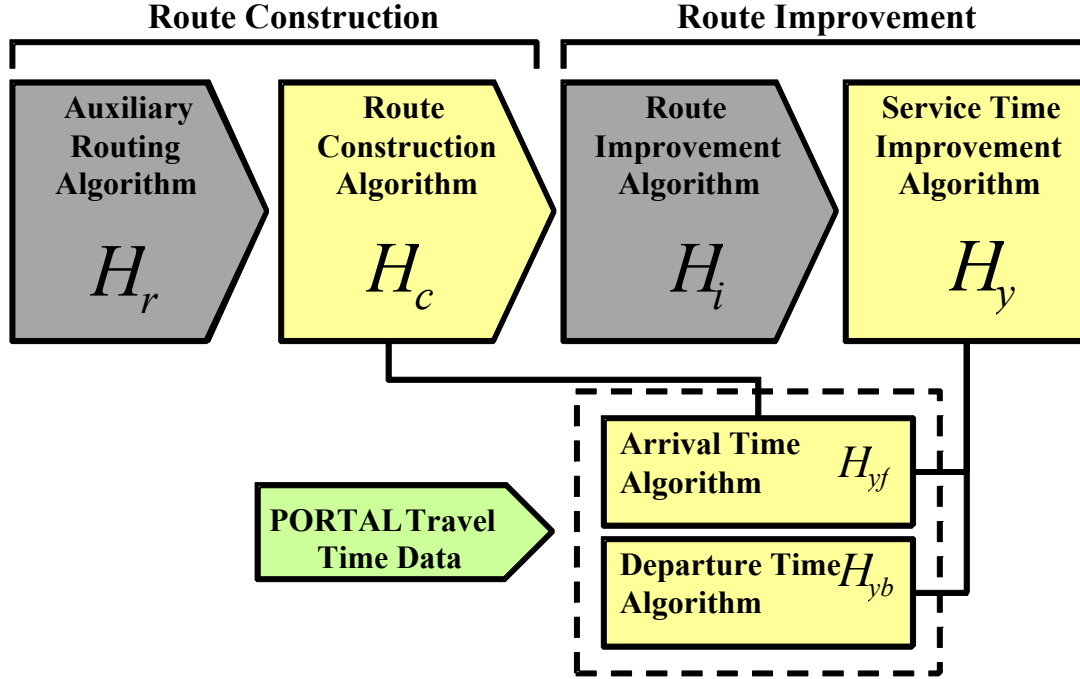
Figure 4: Solution method of the iterative route construction and improvement (IRCI) algorithm.

Although the application of the TDVRP algorithm does not change, it is necessary to develop a travel speed and an emissions calculation sub-algorithm to estimate CO_2 levels as a function of the customer sequence, departure time and road type. The speeds for each time period and path sections, as well as the CO_2 emissions calculation, are calculated as shown in Algorithm H_e. After initializing the variables (line 1), the algorithm calculates a departure time that satisfies time window constraints (lines 2 to 5). Line 6 introduces the loop condition that ensures that the distance between customers is reached. Lines 7 and 8 ensure that the correct section and time period are selected, respectively. Line 9 sets the travel speed to the highest feasible value and line 10 calculates the arrival time after completing the current segment. Lines 11 to 14 calculate emissions if the current segment can be completed in the current interval of time. Otherwise new time periods are utilized until the segment is completed (lines 15 to 23) and emissions are accumulated in line 20. This process is repeated for all road segments between the two customers until all emissions are properly accounted for. According to H_e, the vehicles travel at the fastest possible speed as permitted by congestion and road type.

Algorithm H_e

Data:

$\mathbf{T}$ and $\mathbf{S}$: time intervals and speeds v_i, v_j, a_i, b_i: two customers v_i, v_j served in this order in route k, a_i is the current arrival time at customer i and b_i the proposed departure time

START

1 **initialize** $D \leftarrow 0,\ t \leftarrow 0,\ v_{ij}(b_i) \leftarrow 0$

2 **if** $b_i < \max(e_i, a_i) + g_i$ **then**

3      $b_i \leftarrow \max(e_i, a_i) + g_i,\ t \leftarrow b_i$

4 **else** $t \leftarrow b_i$

5 **end if**

6 **while** $D \leq d_{ij}$ **do**

7   **find** $\min(k')$ such that $D \leq \sum_{1}^{k'} r_{ij}^{k'}$

8   **find** k such that $t_{\underline{k}} \leq t \leq t_{\bar{k}}$

9      $s \leftarrow \bar{s}_{ij}^{k,k'}$

10      $a_{k'} \leftarrow t + r_{ij}^{k'} / s$

11   **if** $a_{k'} < t_{\bar{k}}$ **then**

12          $v_{ij}(b_i) \leftarrow v_{ij}(b_i) +$ formula (15) with speed $s_{kk'}$, distance $r_{ij}^{k'}$

13          $d \leftarrow r_{ij}^{k'}, t \leftarrow \max(b_i, t_{\underline{k}}), D \leftarrow D + r_{ij}^{k'}$

14   **end if**

15   **while** $a_{k'} > t_{\bar{k}}$ **do**

16          $d \leftarrow d - (t_{\bar{k}} - t)s_{kk'}$

17          $D \leftarrow D + (t_{\bar{k}} - t)s_{kk'}$

18          $t \leftarrow t_{\bar{k}}, s_{k+1,k'} \leftarrow \bar{s}_{ij}^{k+1,k'}$

19          $a_{k'} \leftarrow t + d / s_{k+1,k'}$

20          $v_{ij}(b_i) \leftarrow v_{ij}(b_i) +$ formula (15) with speed $s_{k+1,k'}$, distance $(\min(a_{k'}, t_{\bar{k}+1}) - t)s_{k+1,k'}$

21          $k \leftarrow k + 1$

22   **end while**

23 **end while**

24 **END**

25 **Output:**

26      $a_{k'}$, arrival time at customer j

27      $v_{ij}(b_i) = CO_2$ emissions between customers i, j for a departure time b_i

28

5.0 EMISSIONS RESULTS

Three basic scenarios are developed: (1) "uncongested" or base case, (2) "congested" case, and (3) uncongested case but limiting travel speed to 44 miles per hour in freeways – the most efficient travel speed in terms of vehicle CO_2 emissions – and 30 miles per hour in local networks. The latter case (3) is denoted "speed limit-uncongested" case. The average results (i.e., the averages per Solomon problem type) per routing class and for the central depot are presented in tables 1 and 2. Table 1 compares the base "uncongested" case (1) against the "congested" case (2). In tables 1, 2, 3 and 4, the percentage change shown takes the uncongested situation as a base. For example, a positive percentage in the row of routes (or emissions levels) indicates that the average number of required routes (or emissions levels) has increased.

	R1	R2	C1	C2	RC1	RC2
Vehicles	14.9%	22.2%	0.0%	0.0%	13.8%	17.4%
Distance	10.0%	-2.3%	0.0%	0.0%	8.3%	-1.0%
Duration	43.9%	42.6%	40.4%	27.3%	40.1%	43.9%
Emissions	18.2%	4.2%	1.0%	0.8%	17.0%	8.6%

Table 1. Central Depot, Uncongested vs. Congested Case

In Table 1, route durations have an increase across the board due to congestion and longer travel times. Fleet size increases in instances R1, R2, RC1 and RC2 because time windows are the binding constraints. However, fleet size does not change for C1 and C2 problems because vehicle capacity is the binding constraint and the existing fleet of vehicles can serve the same number of customers even under congested conditions. The percentage increase in CO_2 emissions greatly varies across problem types. The highest CO_2 increase is found in R1 and RC1 problems, where customers have tight time windows and larger fleet sizes.

Table 2 compares the "speed limit-uncongested" case against the "uncongested" case. In all cases, the percentage change utilizes the uncongested situation as a base. As expected, duration increases across the board because speed limits have been reduced along the freeway sections. However, it can be observed in Table 2 that emissions may decrease significantly when speed limits are imposed without significantly increasing fleet size (e.g., type R2). In other problems, a CO_2 emissions reduction is achieved with an increase in fleet size and a reduction in distance travel (e.g., type R1). The departure time from the depot is also affected by the speed limit. To reach the first customer within the time window, an earlier departure time may be needed if freeway speeds are reduced or if it is necessary to travel during a congested time period. Hence, traffic congestion or speed limits will have different impacts if customer time windows and depot

location require the usage of congested time periods or time periods where speed limits are binding.

	R1	R2	C1	C2	RC1	RC2
Vehicle	7.4%	0.7%	0.0%	0.0%	0.0%	1.1%
Distance	-5.5%	0.0%	0.0%	0.0%	-0.8%	-0.5%
Duration	4.6%	9.7%	38.0%	24.1%	8.0%	8.3%
Emissions	-13.9%	-4.5%	-25.5%	-17.3%	-4.6%	-4.3%

Table 2. Central Depot, Uncongested vs. Speed Limit-uncongested Case

The average results per routing class and for the suburban depot are presented in tables 3 and 4. Table 3 compares the base "uncongested" case (1) against the "congested" case (2). In all cases, the percentage change shown takes the uncongested situation as a base. As observed in the central depot results, route durations have an increase across the board and fleet size does not change for C1 and C2 problems because vehicle capacity is the binding constraint and the existing fleet of vehicles can serve the same number of customers, even under congested conditions. The percentage increase in CO_2 emissions is in all cases greater than the increases in fleet size or distance traveled because more time is spent travelling on congested network links.

	R1	R2	C1	C2	RC1	RC2
Vehicles	15%	21%	0%	0%	14%	17%
Distance	14%	15%	0%	-1%	13%	12%
Duration	49%	51%	29%	63%	46%	48%
Emissions	23%	28%	8%	9%	21%	23%

Table 3. Suburban Depot, Uncongested vs. Congested Case

Table 4 compares the "speed limit-uncongested" case against the "uncongested" case for the suburban depot. In all cases, the percentage change shown is taking the uncongested situation as a base. As expected, duration increases across the board. It can be observed, again, in Table 4 that emissions may decrease significantly when speed limits are imposed without increasing distance traveled or fleet size (e.g., type C2). In other problems, an emissions reduction is achieved with a slight increase in fleet size or distance traveled (e.g., R1 and RC1 problems, respectively). Comparing tables 2 and 4, it seems that emissions percentage *decreases* are higher for the central depot; to explain this decrease, it is necessary to look at the type of road utilized

22

by the vehicles and the timing of the depot departure in relation to the congested travel periods. Emissions reductions, keeping travel distance constant, can be explained by two factors: (a) the proportion of travel at the optimal speed on the freeway and (b) the proportion of travel on non-freeway segments. Customer time windows and depot locations can affect both factors.

	R1	R2	C1	C2	RC1	RC2
Vehicles	1%	0%	0%	0%	1%	0%
Distance	-1%	0%	0%	0%	1%	0%
Duration	12%	10%	13%	25%	14%	11%
Emissions	-4%	-2%	-1%	-17%	-3%	-2%

Table 4. Suburban Depot, Uncongested vs. Speed Limit-uncongested Case

Travel speed changes can have unexpected consequences even if customer time windows are not included in the analysis. The following example illustrates potential unexpected changes in emissions when speed limits are imposed (see Table 5). Let's assume a freeway speed of 50 mph and a non-freeway (local streets) speed of 25 mph. For the sake of simplicity, let's also assume that the optimal emissions travel speed is 44 mph, producing an emission level of 1.00 unit; at 40 or 50 mph, the emissions level is 1.10 units (10% higher per mile traveled) and at 25 mph the emissions level is producing 1.30 units (30% higher per mile traveled). Let's assume that a route "A" visits all customers traveling 20 miles on freeways and 10 miles on local streets. If freeway speeds were to increase above 50 mph, total emissions in route "A" would increase. If a speed limit on freeways is introduced, route "B", the total amount of emissions will drop to 33 units (5.7%). However, if there is a route duration constraint of 50 minutes, route "B" is not feasible and the next best feasible option, route "C", has a longer duration and distance traveled than route "A". However, total emissions are reduced to 33.2 units (5.3%) because the proportion of freeway travel has increased. Furthermore, if the objective function is to reduce fleet and distance, a suboptimal choice from the emissions perspective will be made if route "D" (with longer travel distance) but less emissions is not chosen. If the reduction of freeway speed is more than is required (congestion), the results are even worse than in the initial starting point (compare route "E" vs. route "A"). Hence, policies that aim to reduce CO_2 emission levels by reducing speed limits will be more successful if (a) freeway travel speeds are at the optimum emissions speed level, (b) the imposition of a speed limit does not increase the proportion of distance traveled in local roads, and (c) the overall distance traveled does not increase. When time windows are present, the analysis is more difficult because the departure time from the depot is also constrained by the speed limit or the timing of the congested period (to reach the first customer within the time window, an earlier departure time may be needed if freeway speeds are reduced or if it is necessary to travel during a congested time period).

Route	Speed		Emission Factors		Distance		Total		
	Freeway	Local	Freeway	Local	Freeway	Local	Distance	Duration	Emissions
A	50.0	25.0	1.1	1.3	20.0	10.0	30.0	48.0	35.0
B	44.0	25.0	1.0	1.3	20.0	10.0	30.0	51.3	33.0
C	44.0	25.0	1.0	1.3	26.0	5.5	31.5	48.7	33.2
D	44.0	25.0	1.0	1.3	27.1	4.5	31.6	47.8	33.0
E	40.0	25.0	1.1	1.3	28.5	3.0	31.5	50.0	35.3

Table 5. Route Comparisons When Speed and Duration Constraints are Introduced

Important emission reductions can be obtained by optimizing travel speeds. However, it should be clear that depot location has a significant role on total level of emissions. To better illustrate this point a new depot, the intermediate depot, is added approximately one-third of the way between the central area and the suburban depot. To simplify comparisons, there are no changes in vehicle fleet size and local distance in tables 6 and 7 because vehicles in the intermediate and suburban depots are allowed to depart earlier and return later. In addition, depots time windows are relaxed so that the same routes are followed. In both tables 6 and 7, the percentage changes utilize the central depot case (uncongested and congested, respectively) as a reference point. Vehicle percentage change is not shown as the fleet sizes are kept constant to facilitate comparisons.

		R1	R2	C1	C2	RC1	RC2
Intermediate Depot	Distance	137%	105%	136%	111%	137%	110%
	Duration	111%	58%	108%	65%	110%	63%
	Emissions	112%	93%	111%	96%	111%	96%
Suburban Depot	Distance	555%	425%	550%	450%	554%	445%
	Duration	449%	233%	436%	263%	446%	256%
	Emissions	327%	272%	325%	283%	327%	281%

Table 6. Urban vs. Intermediate and Suburban Depot (Uncongested conditions)

		R1	R2	C1	C2	RC1	RC2
Intermediate Depot	Distance	137%	105%	136%	111%	137%	110%
	Duration	98%	53%	95%	59%	97%	58%
	Emissions	141%	108%	140%	114%	141%	113%
Suburban Depot	Distance	555%	425%	550%	450%	554%	445%
	Duration	371%	202%	361%	227%	368%	221%
	Emissions	464%	356%	459%	376%	463%	372%

Table 7. Urban vs. Intermediate and Suburban Depot (Congested conditions)

As expected, distances and durations increase across the board if the depot is moved away from the customer service area. In all cases, distance increases more than duration because there is a higher proportion of faster freeway travel when the depot is located farther away. Emission percentage increases are smaller than distance percentages increases in the uncongested case because fast freeway travel produces fewer emissions than slow travel in local/arterial roads. However, in some congested cases emissions can grow faster than distance traveled (Table 7, intermediate depot). In this case, for the intermediate depot, the vehicles are forced to travel the freeway during the most congested time periods to serve the early morning customers (around or before 8 a.m.) or after serving the late afternoon customers (around or right after 4 p.m.). However, for the suburban depot the location is so far that even when vehicles are forced to travel the freeway during the most congested time periods part of the freeway travel takes place under uncongested conditions.

The results presented in this section highlight the fact that the impact of congestion on commercial vehicle emissions may be difficult to forecast. Easier-to-interpret results are obtained if time windows can be partially relaxed so that the same routes are compared. However, some general trends can be observed in all cases. It is clear that uncongested travel speeds tend to reduce emissions on average. Unfortunately, this is not always the case and in some cases the opposite trend could be observed if free-flow speeds are increased beyond the optimal emissions travel speed.

5.1   DISCUSSION

This first part of the report focused on the analysis of CO_2 emissions for different levels of congestion and time-definitive customer demands. The case study used travel time data from an extensive archive of freeway sensors, time-dependent vehicle routing algorithms, and problems-instances with different customer characteristics. The results indicate that congestion impacts on

commercial vehicle emissions are highly significant though difficult to predict. For example, it is shown in this research that it is possible to construct instances where total route distance or duration increases but emissions decrease. Hence, public agencies and highway operators must carefully study the implications of policies that limit travel speeds or increase speed limits, as they may have unintended negative consequences in terms of CO_2 emissions. If travel speeds are reduced to a speed that is "optimal" from an emissions perspective, emissions can be reduced without a significant increase in fleet sizes or distance traveled if the utilization of arterials or local streets does not increase. In addition, the type of objective function (distance, duration or emissions based) used may affect the results.

As a general finding, suburban depots and tight time windows tend to increase emissions on average though the emission increases are affected by several factors, such as duration of the congested period, percentage of freeway travel time traveled under congested conditions, and the difference between free-flow, optimal and congested speeds. From a land use planning and policy perspective, reserving areas for warehousing and distribution activities close to distribution or service areas may significantly decrease commercial CO_2 emissions, especially as congestion levels increase. However, these benefits are not to be expected across the board and may heavily depend on depot locations as well as network and customer demand characteristics. Further research is needed to explore alternative policies to minimize emissions in congested areas without increasing logistics costs or decreasing customer service levels.

6.0 METHODOLOGY TO INCORPORATE REAL-WORLD CONGESTION DATA

The goal of this section is to introduce the methods that can be used to incorporate real-world traffic data and travel times into the problems and algorithms already described in previous sections. A description of the formulation used to estimate LTL routes was presented in Section 3. With hard time window constraints, the primary objective is the minimization of the number of vehicles or routes; the secondary objective is the minimization of the travel time or distance. The TDVRP solution algorithm was presented in Section 4.3; the algorithm consists of a route construction phase and a route improvement phase, each utilizing two separate algorithms. During route construction, the auxiliary routing algorithm H_r determines feasible routes, with the construction algorithm H_c assigning customers and sequencing the routes. Route improvement is done first with the route improvement algorithm H_i, which compares similar routes and consolidates customers into a set of improved routes. Lastly, the service time improvement algorithm H_y eliminates early time window violations, and then reduces the route duration without introducing additional early or late time window violations. These tasks are accomplished by using the arrival time and departure time algorithms H_{yf} and H_{yb}, respectively, and customers are subsequently re-sequenced as necessary. It is with these algorithms that the PORTAL data and shortest-path travel speeds generated by the Google Maps API are inserted into the solution algorithm.

6.1 NOTATION

For the following travel time algorithms, the total depot working time $[e_\#, l_\#]$ is partitioned into a set of p time periods $\mathbf{T_p} = \{T_1, T_2, \dots, T_p\}$. Each traffic bottleneck locations $\beta_m \in \boldsymbol{\beta_n} = \{\beta_1, \beta_2, \dots \beta_n\}$ is assigned the following data at each time partition $T_k \in \mathbf{T_p}$:

- $\mathbf{O_n^p} = [O_{km}]_{p \times n}$: The table of occupancy values for each time period $T_k \in \mathbf{T_p}$ and bottleneck $\beta_m \in \boldsymbol{\beta_n}$
- $\mathbf{U_{n+1}^p} = [U_{km}]_{p \times n+1}$: Table of vehicle flow inflow and outflow rates for each time period and bottleneck locations. The inflow and outflow rates at time period T_k for bottleneck β_m are U_{km} and $U_{k,m+1}$, respectively
- $\mathbf{v_n^p} = [v_{km}]_{p \times n}$: Table of congested travel speeds obtained from PORTAL

All data are collected from PORTAL and the point source location of each traffic bottleneck is assumed to be midway between detector loops. The algorithms also include the following adjustable parameters for each bottleneck location:

- $\bar{R}_m \in \bar{\mathbf{R}}_\mathbf{n} = \{\bar{R}_1, \bar{R}_2, \dots, \bar{R}_m, \dots, \bar{R}_n\}$: A set of initial radius values at time $t = 0$

- $\bar{L}_m \in \bar{\mathbf{L}}_\mathbf{n} = \{\bar{L}_1, \bar{L}_2, \dots, \bar{L}_m, \dots, \bar{L}_n\}$: A set of average vehicle spacing values

- $\bar{O}_m \in \bar{\mathbf{O}}_\mathbf{n} = \{\bar{O}_1, \bar{O}_2, \dots, \bar{O}_m, \dots, \bar{O}_n\}$: A set of threshold occupancy percentages that determine the expected onset of traffic queuing

- $\bar{v}_m \in \bar{\mathbf{v}}_\mathbf{n} = \{\bar{v}_1, \bar{v}_2, \dots, \bar{v}_m, \dots, \bar{v}_n\}$: A set of free-flow speeds

For the sake of readability, the remainder of this subsection contains a complete listing of variable and function definitions as well as notational conventions.

Notational Conventions

$$
\mathbf{A}_\mathbf{n}^\mathbf{p} =
\begin{pmatrix}
A_{11} & A_{12} & \cdots & A_{1m} & \cdots & A_{1n} \\
A_{21} & A_{22} & \cdots & A_{2m} & \cdots & \vdots \\
\vdots & \vdots & \ddots & \vdots & \cdots & \vdots \\
A_{k1} & A_{k2} & \cdots & A_{km} & \cdots & A_{kn} \\
\vdots & \vdots & \cdots & \vdots & \ddots & \vdots \\
A_{p1} & A_{p2} & \cdots & A_{pm} & \cdots & A_{pn}
\end{pmatrix}
: \text{A matrix with } p \text{ rows and } n \text{ columns}
$$

$\mathbf{A}_\mathbf{n} = \{A_1, A_2, \dots, A_m, \dots, A_n\}$: Row vector with n elements

$$
\mathbf{A}^\mathbf{p} =
\begin{Bmatrix}
A_1 \\
A_2 \\
\vdots \\
A_k \\
\vdots \\
A_p
\end{Bmatrix}
: \text{Column vector with } p \text{ elements}
$$

$\mathbf{A}_\mathbf{m} \cup A_{m+1} \equiv \{A_1, A_2, \dots, A_m\} \leftarrow A_{m+1} = \{A_1, A_2, \dots, A_m, A_{m+1}\}$

$$
\mathbf{A}_\mathbf{m}^\mathbf{p} \cup \mathbf{A}^\mathbf{p} \equiv
\begin{pmatrix}
A_{11} & A_{12} & \cdots & A_{1m} \\
A_{21} & A_{22} & \cdots & \vdots \\
\vdots & \vdots & \ddots & \vdots \\
A_{p1} & \cdots & \cdots & A_{pm}
\end{pmatrix}
\leftarrow
\begin{pmatrix}
A_1 \\
A_2 \\
\vdots \\
A_p
\end{pmatrix}
=
\begin{pmatrix}
A_{11} & A_{12} & \cdots & A_{1m} & A_{1,m+1} \\
A_{21} & A_{22} & \cdots & A_{2m} & A_{2,m+1} \\
\vdots & \vdots & \ddots & \vdots & \vdots \\
A_{p1} & \cdots & \cdots & A_{pm} & A_{p,m+1}
\end{pmatrix}
$$

$A_m \in \mathbf{A}_\mathbf{n}$: m^{th} element of a row vector with n elements
$A_k \in \mathbf{A}^\mathbf{p}$: k^{th} element of a column vector with p elements
$A_{km} \in \mathbf{A}_\mathbf{n}^\mathbf{p}$: element in the kth row and m^{th} column of a $p \times n$ matrix (p rows and n columns)

Variables	Definition
i, j, m	Indices for set of consecutive customers (i, j) and bottlenecks (m)
$\beta_i = (x_i, y_i); \; \beta_j = (x_j, y_j); \; \beta_m = (x_m, y_m)$	Geographic coordinates of customer i, customer j and bottleneck m, respectively
a_j	Arrival time at customer j
b_i	Departure time from customer i
e_i	Lower time window for customer i
g_i	Service time at customer i
d	Iterated driving distance variable
d_{ij}	Driving distance between customers i and j calculated by the Google Maps API
t_{ij}	Free-flow travel time between customers i and j calculated by the Google Maps API
$u_{ij} = \dfrac{d_{ij}}{t_{ij}}$	"Free-flow" speed used in TDVRP algorithm
Array/Vector quantities	**Definition**
$T_k \equiv [t_{\bar{k}}, t_{\underline{k}}] \in \mathbf{T_p} = \{T_1, T_2, \dots T_p\},$	Set of time periods as fraction of depot working time
$\bar{R}_m \in \bar{\mathbf{R}}_\mathbf{n} = \{\bar{R}_1, \bar{R}_2, \dots, \bar{R}_n\}$	A set of initial radius values at each bottleneck location at time $t = 0$
$\bar{L}_m \in \bar{\mathbf{L}}_\mathbf{n} = \{\bar{L}_1, \bar{L}_2, \dots, \bar{L}_n\}$	A set of average vehicle spacing values for each bottleneck location
$\bar{O}_m \in \bar{\mathbf{O}}_\mathbf{n} = \{\bar{O}_1, \bar{O}_2, \dots, \bar{O}_n\}$	A set of threshold occupancy percentages that determine the expected onset of traffic queuing
$\bar{v}_m \in \bar{\mathbf{v}}_\mathbf{n} = \{\bar{v}_1, \bar{v}_2, \dots, \bar{v}_n\}$	Bottleneck speed parameters
$U_{km}, U_{k,m+1} \in \mathbf{U}_{\mathbf{n+1}}^{\mathbf{p}} = [U_{km}]_{p \times n+1}$	Table of vehicle flow inflow and outflow rates for each time period and bottleneck
$\mathbf{O}_\mathbf{n}^\mathbf{p} = [O_{km}]_{p \times n}$	Table of occupancy values for each time period and bottleneck
$\mathbf{v}_\mathbf{n}^\mathbf{p} = [v_{km}]_{p \times n}$	Speed at bottleneck B_m for the kth time period entered as a $p \times n$ array
Functions	**Definition**
$f(x_\mu, x_v, y_\mu, y_v)$	Euclidean distance between two sets of x-y coordinates

6.2   TRAFFIC QUEUING ALGORITHM

The following is a summary of the H_{yc} algorithm that assembles a table of bottleneck radii R_{km} for each bottleneck β_m and time period T_k. The algorithm requires the input data arrays $\mathbf{O}_n^p$ and $\mathbf{U}_{n+1}^p$ as well as the adjustable parameters $\mathbf{\bar{R}_n}$, $\mathbf{\bar{L}_n}$ and $\mathbf{\bar{O}_n}$. The output table $\mathbf{R}_n^p$ contains the radius value for each time period T_k at each bottleneck β_m in a $p \times n$ array. The complete pseudo-code is provided in the Appendix; beginning with the conditional statement within the nested for-loop for a particular β_m and starting at $t = 0$, the algorithm can be described as follows:

1. First assign the variable R the base parameter value $\bar{R}_m$ at $t = 0$

2. Begin the k iteration; if the occupancy O_{km} at a given k iteration is greater than the threshold value $\bar{O}_m$, add the differences in the outflow and inflow traffic volumes multiplied by the duration of the time partition $t_{\bar{k}} - t_{\underline{k}}$ by the average vehicle spacing $\bar{L}_m$ to the variable R

3. If the occupancy O_{km} is less than $\bar{O}_m$ and the radius variable R is greater than the base parameter $\bar{R}_m$, then subtract the quantity from step 2 from R

4. Take the maximum of the set $[R, \bar{R}_m]$; this and the second condition of step 3 prevent R from being assigned a negative value and ensures that $\bar{R}_m$ is a lower bound for the variable R when the predicted traffic queue is dispersing

5. Otherwise, retain $R = \bar{R}_m$

6. Construct a column vector $\mathbf{R^p}$ of R values obtained from each k iteration

7. Repeat steps 1 through 6 n times and construct the output matrix $\mathbf{R}_n^p$ from the column vectors $\mathbf{R^p}$ obtained from each iteration.

In summary, the H_{yr} algorithm adds or subtracts expected lengths of traffic queues to the radius of the effective area of each bottleneck, which is dependent on whether the measured occupancy is above or below each threshold value contained in $\mathbf{\bar{O}_n}$. The table of values in $\mathbf{R}_n^p$ is referenced by the H_{yf} and H_{yb} algorithms described in detail in the following section. The objective is to extrapolate travel time trends from the data that are available and apply them to the surrounding road network.

6.3 ARRIVAL AND DEPARTURE TIME ALGORITHMS

The following is a summary of the arrival time and departure time algorithms H_{yf} and H_{yb} that estimate travel times between pairs of customers β_i and β_j using the travel time data. The H_{yf} algorithm calculates the expected arrival time at a customer β_j when departing from a previous customer β_i using a forward-iterative process. Similarly, the H_{yb} algorithm utilizes a backward iterative process and simultaneously calculates the required departure time from customer β_i to reach customer β_j.

The impact of bottlenecks as vehicles are moving through different periods of time is a function of the estimated distance between the vehicle and the bottleneck at the beginning of each time period. A linear approximation of the vehicle location is used to reduce computational complexity because shortest path and Euclidean distances are highly correlated. High levels of correlation between Euclidian and shortest-path distances are usually found in urban areas. The distance traveled along the Euclidean connecting line is calculated as a percentage of the actual route traversed such that

$$d' = \frac{d}{d_{ij}} D_{ij}. \tag{1}$$

Using the law of cosines (see Figure 5), the distance from a point on the Euclidian connecting line to each bottleneck at a given time iteration in the forward iterative calculation can be shown to be

$$r_m = \sqrt{\left(\frac{d}{d_{ij}} D_{ij}\right)^2 + D_{jm}^2 - \frac{d\left(D_{ij}^2 + D_{jm}^2 - D_{im}^2\right)}{d_{ij}}}. \tag{2}$$
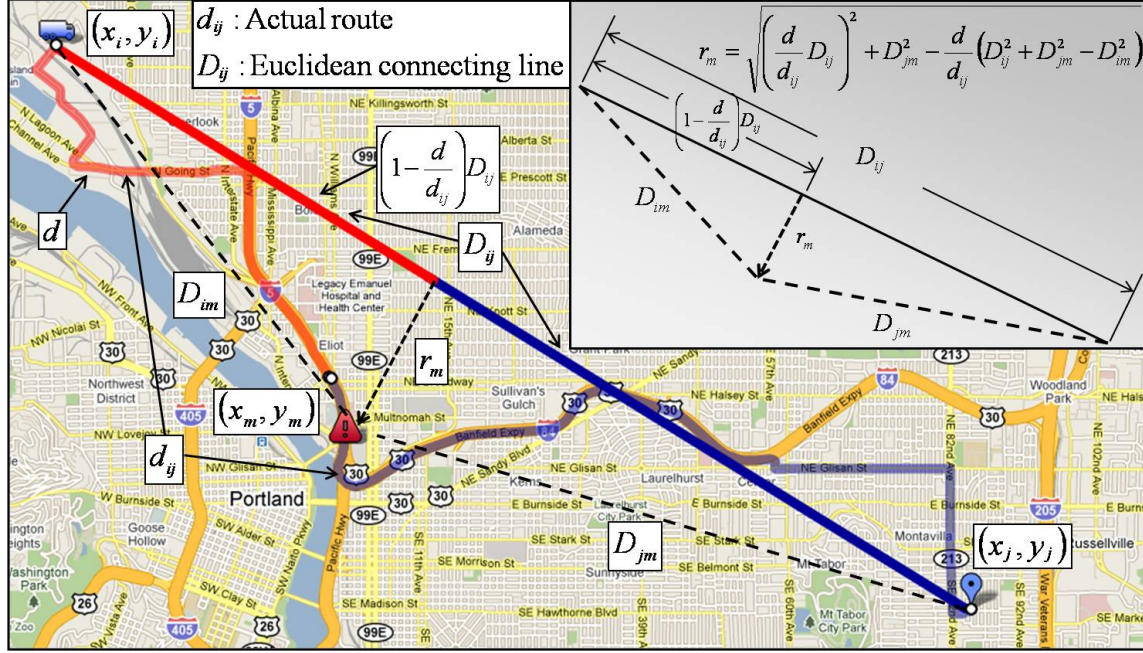
Figure 5: Illustration of the method to approximate bottleneck influence

Similarly for the backwards iterative process of the departure time algorithm, the distance from the nearest bottleneck is

$$r_m = \sqrt{\left(\frac{d}{d_{ij}} D_{ij}\right)^2 + D_{im}^2 - \frac{d\left(D_{ij}^2 + D_{im}^2 - D_{jm}^2\right)}{d_{ij}}}.$$

In the previous equations D_{ij}, D_{im}, and D_{jm} are the Euclidean distances between customers i and j; customer i and bottleneck β_m; and customer j and bottleneck β_m, respectively; d_{ij} is the shortest-path driving distance from customer i to customer j calculated by the API; and d is the iterated distance from i to j along the actual driving route. A derivation of this function can be found in the next subsections. Other algorithms are found in the Appendix.

6.4   DERIVATION OF BOTTLENECK DISTANCE

The following is the derivation of the bottleneck distance function r for the forward-iterative calculation in the AT algorithm. An identical argument with the distance d iterated in the backward direction from a customer j to i obtains the bottleneck distance function for the DT algorithm in a trivial manner.

Let θ_{im} be the angle opposite D_{im}, the Euclidean distance from customer i to bottleneck B_m. Using the law of cosines:

$$D_{im}^2 = D_{ij}^2 + D_{jm}^2 - 2D_{ij}D_{jm}\cos(\theta_{im}).$$

$$\cos(\theta_{im}) = \frac{D_{ij}^2 + D_{jm}^2 - D_{im}^2}{2D_{ij}D_{jm}}.$$

θ_{im} is also the angle opposite to r; equating r and equation **Error! Reference source not found.**) and using the law of cosines again:

$$r_m^2 = \left(\frac{d}{d_{ij}}D_{ij}\right)^2 + D_{jm}^2 - 2\left(\frac{d}{d_{ij}}D_{ij}\right)D_{jm}\cos(\theta_{im})$$

$$= \left(\frac{d}{d_{ij}}D_{ij}\right)^2 + D_{jm}^2 - 2\left(\frac{d}{d_{ij}}D_{ij}\right)D_{jm}\left(\frac{D_{ij}^2 + D_{jm}^2 - D_{im}^2}{2D_{ij}D_{jm}}\right)$$

$$= \left(\frac{d}{d_{ij}}D_{ij}\right)^2 + D_{jm}^2 - \frac{d}{d_{ij}}\left(D_{ij}^2 + D_{jm}^2 - D_{im}^2\right)$$

$$\Rightarrow r_m = \sqrt{\left(\frac{d}{d_{ij}}D_{ij}\right)^2 + D_{jm}^2 - \frac{d}{d_{ij}}\left(D_{ij}^2 + D_{jm}^2 - D_{im}^2\right)}$$

6.5   SUMMARY

The travel speed function s_m is applied at each time iteration T_k and calculates a speed value for each bottleneck. This function calculates congested travel speeds s_m as reductions in the API-derived speed u_{ij} proportional to the speed reduction measured at the traffic bottlenecks such that $\frac{s_m}{u_{ij}} = \frac{v_{km}}{\bar{v}_m}$ if the virtual location on the Euclidean connecting line is within the radius R_{km}. Here v_{km} is the time-varying speed obtained from PORTAL and $\bar{v}_m$ is an adjustable parameter that may represent the freeway free-flow speed. In other words, the reduction in travel speed due to congestion in the surrounding network is assumed to be proportional to the reduction observed from the PORTAL freeway data at the bottleneck (detector station) with the slowest travel speed. This function can be expressed as

$$s_m = \begin{cases} \dfrac{u_{ij} v_{km}}{\bar{v}_m} & r_m \leq R_{km} \\ u_{ij} & r_m > R_{km} \end{cases}$$

where r_m is the distance from a point along the Euclidean connecting line to a bottleneck β_m.

The following is a summary of the $\boldsymbol{H_{yf}}$ algorithm; the pseudo-code can be found in the Appendix:

1. First determine if the arrival time a_i is less than the lower time window e_i at customer i
   a. If so, then the vehicle waits and the expected departure time is e_i plus the service time g_i
   b. If not, then the departure time is simply the arrival time plus the service time
2. Determine k for the discrete time period T_k with bounds $[t_{\underline{k}}, t_{\bar{k}}]$ that the expected departure time b_i lies in. This is the initial value for the iterator in the while loop
3. Determine the Euclidean distance of each traffic bottleneck to the location $\beta_i = (x_i, y_i)$ of customer i; the speed function is calculated for each value m and a row vector $\mathbf{S_n}$ of speeds is assembled. The initial travel speed of the vehicle in the subsequent forward-iterative process is calculated as the minimum value of $\mathbf{S_n}$ (i.e., the travel speed is only as fast as that imposed by the bottleneck) with the worst travel speed only among the subset of bottlenecks whose area of influence affects the path between customers at a given time.
4. Terminate the while loop when the vehicle has reached its destination. In each period, speeds are recalculated and distances accumulated until the vehicle has reached its destination

Output: the expected arrival time a_j at customer j when departing from customer i at time b_i.

The $\boldsymbol{H_{yb}}$ algorithm works in a similar fashion; given a customer j at location v_j with an expected arrival time a_j obtained from the $\boldsymbol{H_{yf}}$ algorithm, determine the required departure time b_i from customer i at location β_i to make the trip between β_i and β_j without allowing for late time window violations.

Travel times can be calibrated by adjusting $\bar{\mathbf{R}}_{\mathbf{n}}, \bar{\mathbf{L}}_{\mathbf{n}}, \bar{\mathbf{O}}_{\mathbf{n}}, \bar{\mathbf{v}}_{\mathbf{n}}$ parameters as well as the time-dependent travel speeds provided by PORTAL ($\mathbf{v_n^p}$). Directional and time-of-day effects can be incorporated. Memory requirements are reduced because the algorithms work with one travel

time and distance matrix. Simple linear functions and intuitive parameters are used to adapt free-flow travel times to congested conditions.

7.0 PORTLAND APPLICATION

The recurrent effects of traffic congestion at peak periods present daily challenges to LTL carriers in the Portland metropolitan area. The numerical analysis presented in this section aims to represent the above mentioned conditions. Customer data and depot locations are generated using a land use zoning map of the Portland metropolitan area.

7.1 CONGESTION DATA SOURCES

Two main data sources were utilized in this research: Google Maps API for the implementation of the TDVRP algorithm and PORTAL for obtaining historical travel time data. These two sources are described in the following subsections.

The use of the Google Maps API allows access to up-to-date street network data in the studied region with a high level of geographical detail. The open-source nature of the application also allows for considerable freedom in modifying the program and user interface. Figure 6 shows the process of creating customer distributions and obtaining optimized routes from the TDVRP algorithm as implemented with the API. The API consists of several interfaces:

- A customer selection screen where a set of customers and a single depot can be created by clicking on locations on the map. A coordinate output is provided that is then copied into a text (.txt) file.

- An interface that calculates the shortest paths between pairs of customers and constructs the distance and travel time Origin-Destination (O-D) matrices. Distance and travel time matrices are estimated and stored as text files.

- Travel speed, occupancy and vehicle flow data from traffic sensors are used to incorporate the impact of congestion on travel times.

- A solution interface where solution sets outputted from the TDVRP algorithm can be loaded and plotted to provide a visual verification of results.
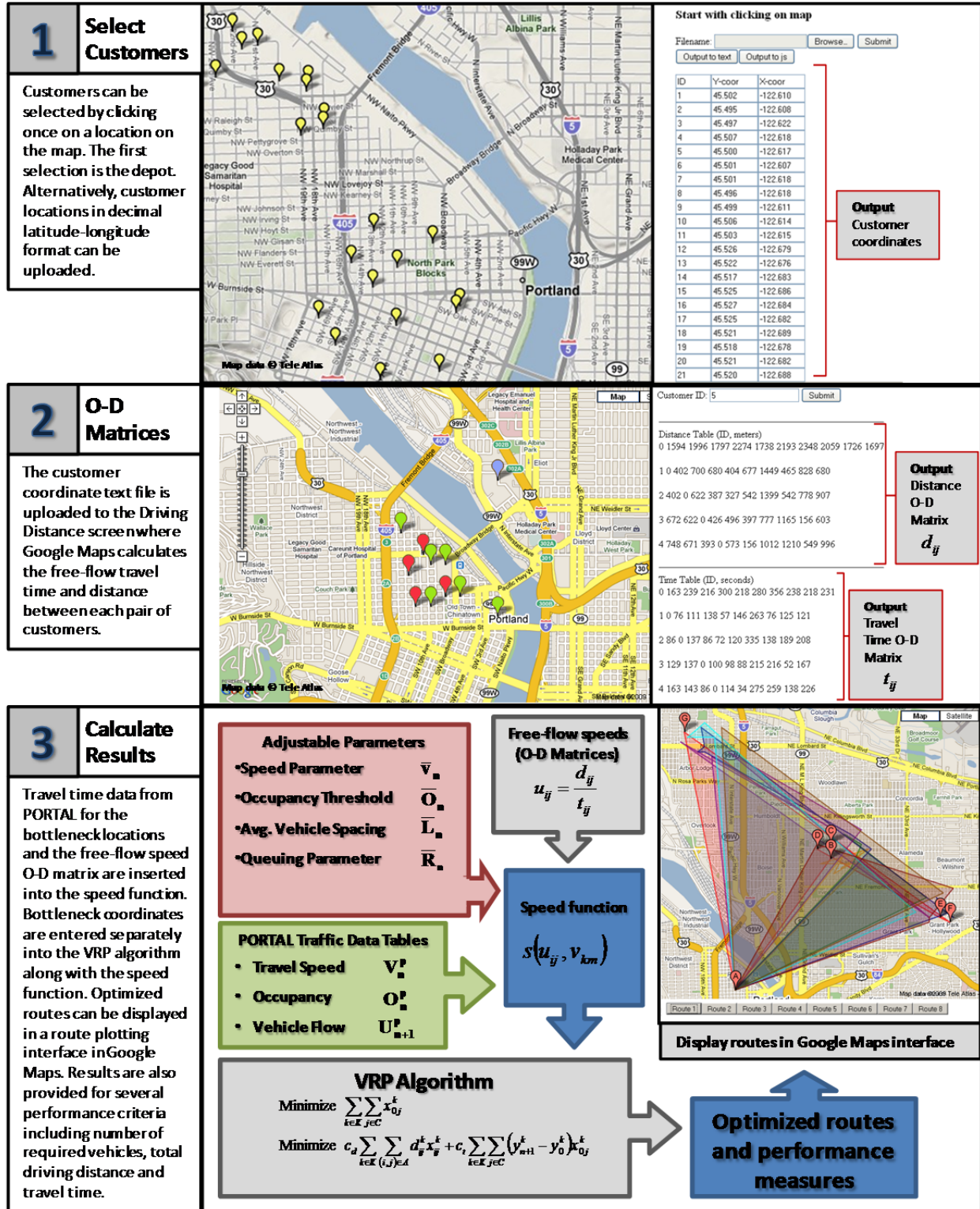
1 Select Customers

Customers can be selected by clicking once on a location on the map. The first selection is the depot. Alternatively, customer locations in decimal latitude-longitude format can be uploaded.

Start with clicking on map

Filename: [ ] [Browse...] [Submit]
[Output to text] [Output to js]

ID	Y-coor	X-coor
1	45.502	-122.610
2	45.495	-122.608
3	45.497	-122.622
4	45.507	-122.618
5	45.500	-122.617
6	45.501	-122.607
7	45.501	-122.618
8	45.496	-122.618
9	45.499	-122.611
10	45.506	-122.614
11	45.503	-122.615
12	45.526	-122.679
13	45.522	-122.676
14	45.517	-122.683
15	45.525	-122.686
16	45.527	-122.684
17	45.525	-122.682
18	45.521	-122.689
19	45.518	-122.678
20	45.521	-122.682
21	45.520	-122.688

Output Customer coordinates

2 O-D Matrices

The customer coordinate text file is uploaded to the Driving Distance screen where Google Maps calculates the free-flow travel time and distance between each pair of customers.

Customer ID: 5 [Submit]

Distance Table (ID, meters)
0 1594 1996 1797 2274 1738 2193 2348 2059 1726 1697

1 0 402 700 680 404 677 1449 465 828 680

2 402 0 622 387 327 542 1399 542 778 907

3 672 622 0 426 496 397 777 1165 156 603

4 748 671 393 0 573 156 1012 1210 549 996

Output Distance O-D Matrix d_{ij}

Time Table (ID, seconds)
0 163 239 216 300 218 280 356 238 218 231

1 0 76 111 138 57 146 263 76 125 121

2 86 0 137 86 72 120 335 138 189 208

3 129 137 0 100 98 88 215 216 52 167

4 163 143 86 0 114 34 275 259 138 226

Output Travel Time O-D Matrix t_{ij}

3 Calculate Results

Travel time data from PORTAL for the bottleneck locations and the free-flow speed O-D matrix are inserted into the speed function. Bottleneck coordinates are entered separately into the VRP algorithm along with the speed function. Optimized routes can be displayed in a route plotting interface in Google Maps. Results are also provided for several performance criteria including number of required vehicles, total driving distance and travel time.

Adjustable Parameters
- Speed Parameter $\overline{v}_\blacksquare$
- Occupancy Threshold $\overline{O}_\blacksquare$
- Avg. Vehicle Spacing $\overline{L}_\blacksquare$
- Queuing Parameter $\overline{R}_\blacksquare$

Free-flow speeds (O-D Matrices)
$$u_{ij} = \frac{d_{ij}}{t_{ij}}$$

PORTAL Traffic Data Tables
- Travel Speed $V_\blacksquare^\blacksquare$
- Occupancy $O_\blacksquare^\blacksquare$
- Vehicle Flow $U_{\blacksquare+1}^\blacksquare$

Speed function $s(u_{ij}, v_{km})$

VRP Algorithm

Minimize $\sum_{k\in K}\sum_{j\in C} x_{0j}^k$

Minimize $c_d \sum_{k\in K}\sum_{(i,j)\in A} d_{ij}^k x_{ij}^k + c_t \sum_{k\in K}\sum_{j\in C}(y_{n+1}^k - y_0^k)x_{0j}^k$

Display routes in Google Maps interface

[Route 1] [Route 2] [Route 3] [Route 4] [Route 5] [Route 6] [Route 7] [Route 8]

Optimized routes and performance measures

Figure 6: Overview of the TDVRP solution methodology and integration of the Google Maps API

38

Perhaps the greatest advantage of the API is that the open-source software and high-quality network data can be accessed free of charge[2]. This, together with the TDVRP solution algorithm developed to interface with the API, offers the potential for very low-cost solutions for route planning and optimization while accessing detailed and accurate network data such as road hierarchy and restrictions (e.g., one-way streets or no-left turn movements at intersections). The effects of congestion are included by modifying the travel times initially calculated by Google Maps. After the TDVRP algorithm design the routes, the API interface can be utilized to obtain detailed driving directions.

7.2   SIMULATING CONGESTION EFFECTS

Google Maps already provides reasonable travel time estimations during uncongested periods. However, to increase the accuracy of travel time estimations, highway sensor data are utilized. For example, segments along I-5 located in proximity to traffic bottlenecks are selected to represent areas of decreased travel speed. The selected segments are between freeway interchanges and/or on/off-ramps where vehicle detector loops are located.

Detailed traffic data are obtained from PORTAL, Portland's implementation of an Archived Data User Service (ADUS), which coordinates and obtains data from approximately 436 inductive loop detectors along interstate freeways in the Portland metropolitan area. Bottlenecks are modeled as point locations surrounded by areas of reduced travel speed. Travel in proximity to a bottleneck is expressed as a percentage reduction in travel speed proportional to the speed reduction at the bottleneck location. Figure 7 shows the bottleneck locations and areas of effective travel speed reduction.
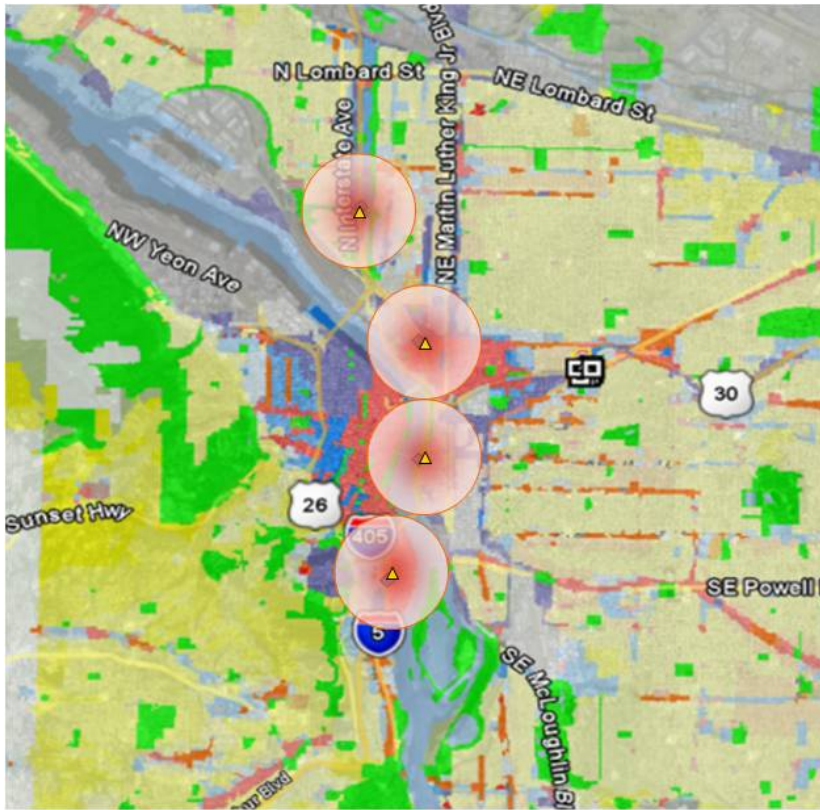
---

[2] http://code.google.com/apis/maps/

Figure 7: Example with bottleneck locations and areas of effective travel speed reduction

Data obtained from PORTAL are also used to model the impacts of traffic queuing on the surrounding network. The areas of reduced travel speed for each bottleneck location are assumed as a function of the measured occupancy and vehicle inflow and outflow rates at each bottleneck location. Research has shown that traffic queues often begin to form at occupancies approximately equal to or greater than 20%, but according to speed-flow data, queues may form at occupancies as low as 13%. Utilizing these queuing concepts and assumptions, the radius of the area of travel speed reduction around each bottleneck, where vehicle travel speed reduced is varied in proportion to the difference in the inflow and outflow rates, multiplied by average vehicle spacing when the occupancy is above a certain threshold value. Strictly, this assumes that there is conservation of vehicles (i.e., no vehicles enter or exit the road segment in question) and ignores the presence of moving traffic queues.

The travel speeds used in this research are calculated from 15-minute archived travel time data averaged over 2007 along the I-5 freeway corridor spanning from the Portland suburb of

Wilsonville to Vancouver, WA. These data are sufficient for purposes of demonstrations of the proposed methodology, but consideration of seasonal or monthly variability in travel time is important for many LTL carriers and is entirely feasible via PORTAL. In this research it is assumed that carriers only account for recurrent congestion and plan their routes the night before making the deliveries.

To test the model using real-world constraints, two delivery periods are modeled and analyzed: (1) An early-morning delivery period that avoids most of the morning peak-hour traffic congestion but with tighter time windows; and (2) an extended morning delivery time that increases the feasible working time but with increased travel during morning peak-hour. **Error! Reference source not found.** provides a qualitative comparison of the simulated delivery times.

A total of 50 customer locations are utilized (Figure 8), with constraints assigned according to the zoning criteria. All customers normally served after 9 a.m. are assumed to be able to shift delivery times prior to this time. Time windows of 15 minutes are randomly assigned to all customer types. Additionally, deliveries to all customers in mixed-use and residential areas are prohibited before 7 a.m. to model required compliance with local noise ordinances. In the early-morning delivery option, this reduces the effective depot working time to just two hours for these customers. The extended morning delivery option provides a four-hour working time for these customers, but includes the effects of the morning peak-hour congestion to a greater degree. The calibration of the model was tested by varying the travel speed parameters $\bar{v}_n$ to alter the simulated travel speed derived from the PORTAL travel time data and contained in the travel speed table v_n^p.
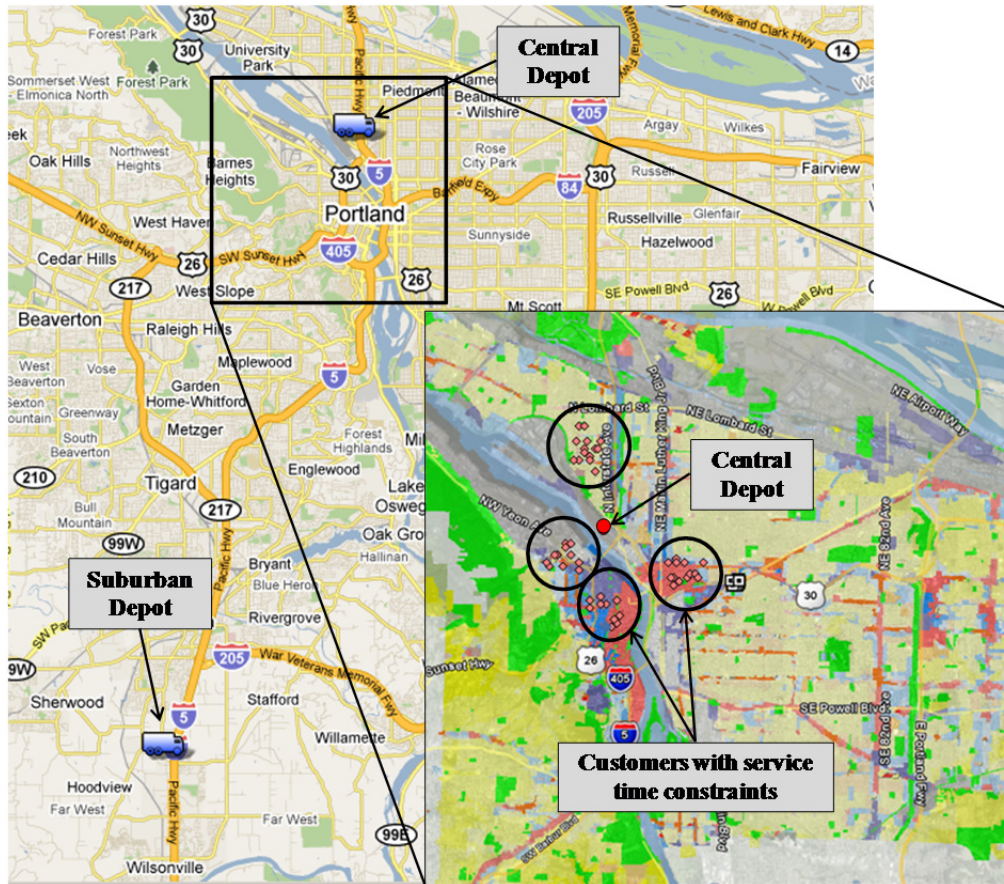
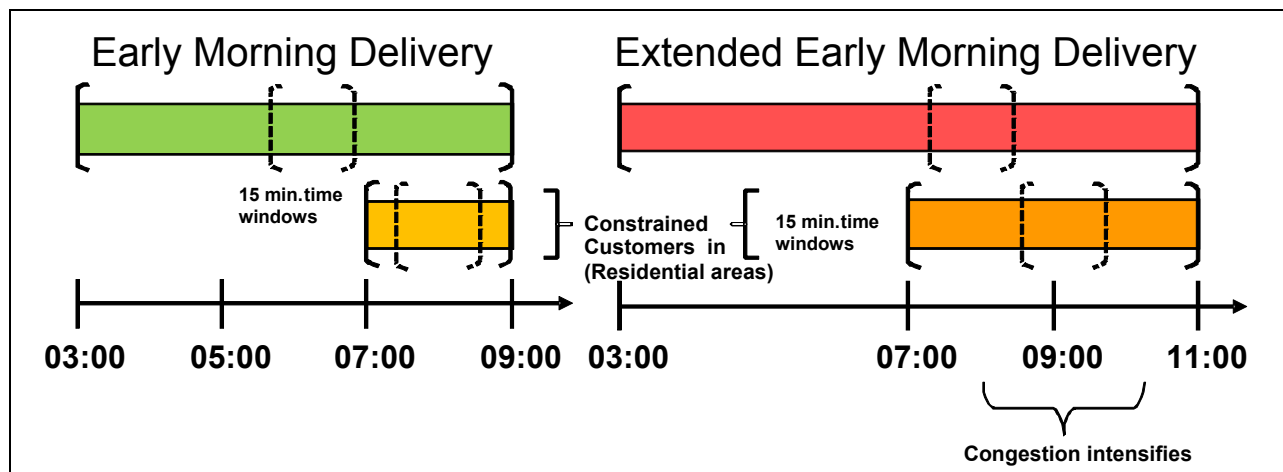Figure 8: Customer service area and depot locations

Figure 9: Modeled delivery periods, constrained customers and time window constraints

8.0 EXPERIMENTAL RESULTS

Results comparing the number of vehicles and total distance traveled during the morning and extended morning delivery periods are presented in this section. In addition, to incorporate the impact of travel time reliability, time-varying travel speed from PORTAL are decreased by a coefficient δ. This adjustment maintains the overall trend in travel speed variation throughout the delivery period, but allows for adjustments to the travel time to more accurately reflect real-world differences between *average* travel speeds and the actual *distribution* of travel speeds. A value $\delta = 1$ utilizes *average* time-varying travel speed PORTAL data and assumes that no hard time window violations take place if realized travel times are at least the average travel speed. However, if the carriers would like to account for travel time unreliability a value of $\delta < 1$ can be used in the calculations as follows:

$$
s_m = \begin{cases} \delta \dfrac{u_{ij} v_{km}}{\bar{v}_m} & r_m \leq R_{km} \\ u_{ij} & r_m > R_{km} \end{cases}
$$

A value of $\delta < 1$ guarantees a higher value of customer service. The sensitivity to travel time unreliability and buffer times was tested by setting the parameter $\delta = \{0.4, 0.6, 0.8, 1\}$.

8.1 IMPACT OF CONGESTION ON THE NUMBER OF VEHICLES

For the number of required vehicles (Figure 10), the central depot showed less sensitivity to changes in travel time reliability than the suburban depot. As expected, reduced travel speed appears to have a greater impact on fleet size when the depot has a suburban location. The number of vehicles required is consistently less for the extended early-morning delivery period and a larger fleet is still required when the depot has a suburban location.
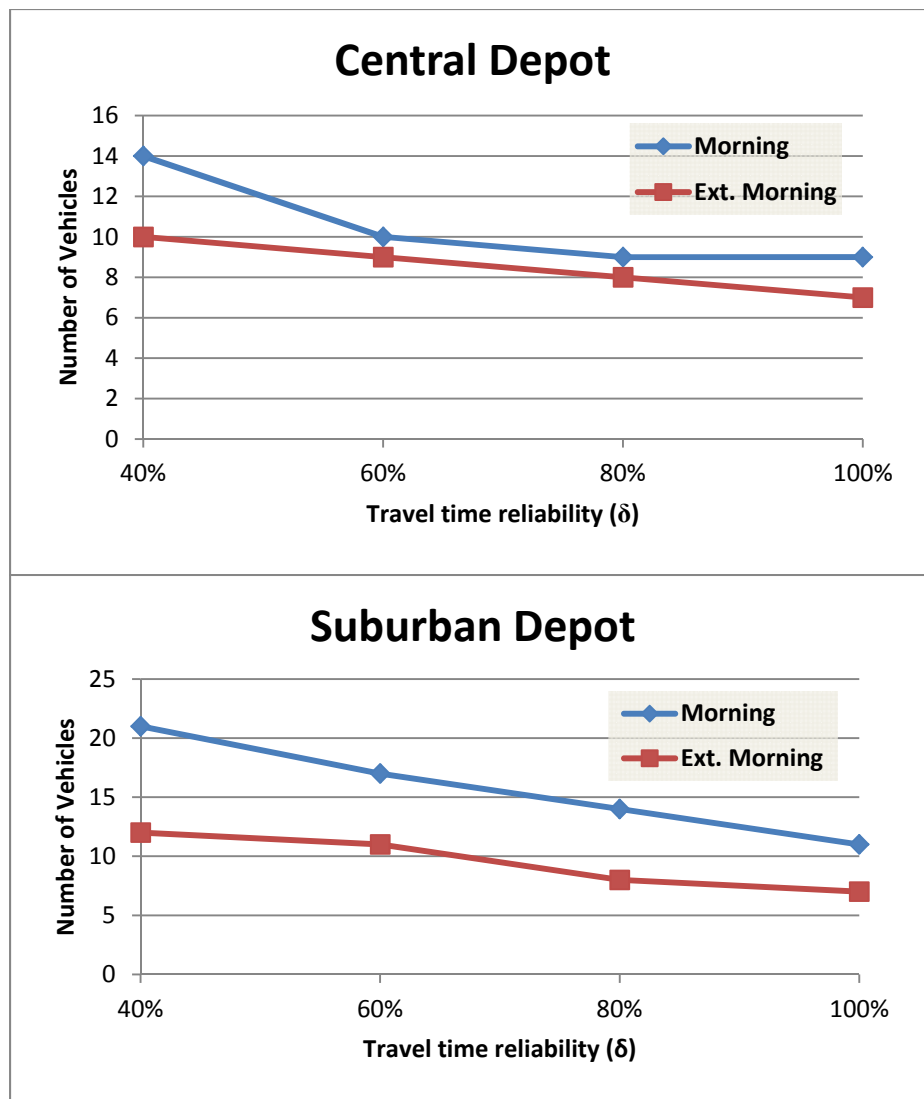
Figure 10: Effects of congestion on fleet size

8.2   IMPACT OF CONGESTION ON THE TOTAL DISTANCE TRAVELED

Comparisons of total vehicle miles traveled (VMT) are provided in Figure 11. Similar to the required number of vehicles, total VMT is significantly higher for tours originating at the suburban depot location. Constrained service times for customers in the early-morning delivery period also appear to impact total VMT to a slightly greater extent than travel speed.
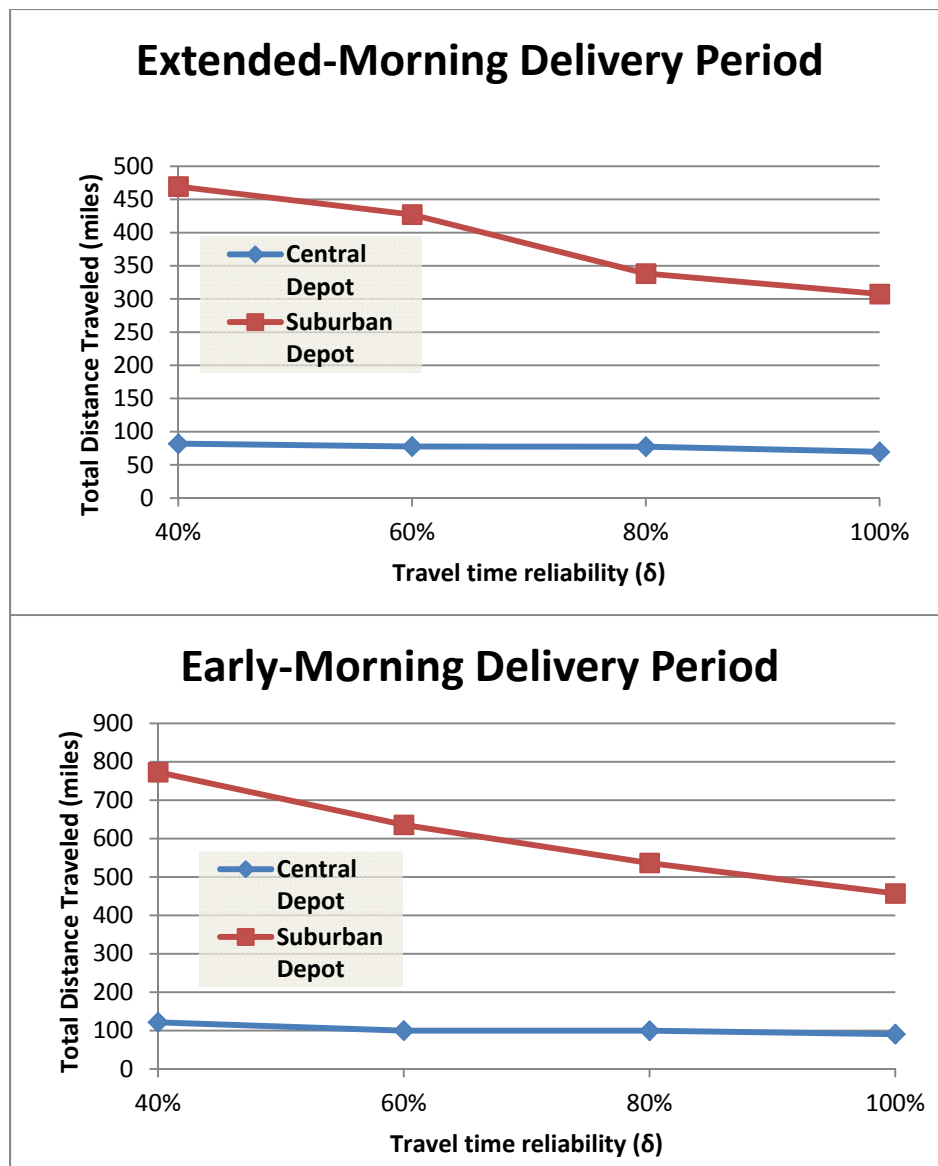
Figure 11: Effects of congestion on total VMT

8.3   DISCUSSION

This research proposes a new methodology for integrating real-world road networks and travel data to time-dependent vehicle routing solution methods. The use of traffic sensor data and Google Maps API provides a unique approach to interface routing algorithms, travel time and congestion data. Intuitive algorithms and parameters are used to incorporate the impacts of congestion on time-dependent travel time matrices. The proposed methodology is a significant improvement in terms of representing the impacts of congestion in urban areas, leveraging on existing open source data and applications.

45

The results show the dramatic impacts of congestion on carriers' fleet sizes and distance traveled. The results also suggest that congestion has a significant impact on fleet size, particularly for depots located in suburban areas outside of the customer service area.

9.0   REFERENCES

AHN, B. H. & SHIN, J. Y. (1991) Vehicle-routing with time windows and time-varying congestion. *Journal of the Operational Research Society,* 42(5)**,** 393-400.

BARTH, M. & BORIBOONSOMSIN, K. (2008) Real-World Carbon Dioxide Impacts of Traffic Congestion. *Transportation Research Record 2058***,** 163-171.

BAUMGARTNER, M., LÉONARDI, J. & KRUSCH, O. (2008) Improving computerized routing and scheduling and vehicle telematics: A qualitative survey. *Transportation Research Part D,* 13(6)**,** 377-382.

BERTINI, R. L., HANSEN, S., MATTHEWS, S., RODRIGUEZ, A. & DELCAMBRE, A. (2005) PORTAL: Implementing a New Generation Archive Data User Service in Portland, Oregon. *12th World Congress on ITS,* 1976(November).

CONRAD, R. & FIGLIOZZI, M. A. (2010) Algorithms to Quantify the Impacts of Congestion on Time-Dependent Real-World Urban Freight Distribution Networks. *Transportation Research Record 2168*, p.104-113.

CORDEAU, J. F., LAPORTE, G., SAVELSBERGH, M. & VIGO, D. (2006) Vehicle Routing. IN BARNHART, C. & LAPORTE, G. (Eds.) *Transportation, Handbooks in Operations Research and Management Science.* Amsterdam, North-Holland.

CRAINIC, T. G., RICCIARDI, N. & STORCHI, G. (2004) Advanced freight transportation systems for congested urban areas. *Transportation Research Part C: Emerging Technologies,* 12(2)**,** 119.

CRAINIC, T. G., RICCIARDI, N. & STORCHI, G. (2009) Models for Evaluating and Planning City Logistics Systems. *Transportation Science,* 43(4)**,** 432-454.

DESROCHERS, M., LENSTRA, J. K., SAVELSBERGH, M. W. P. & SOUMIS, F. (1988) Vehicle routing with time windows: optimization and approximation. *Vehicle Routing: Methods and Studies,* 16(65-84.

DONATI, A. V., MONTEMANNI, R., CASAGRANDE, N., RIZZOLI, A. E. & GAMBARDELLA, L. M. (2008) Time dependent vehicle routing problem with a multi ant colony system. *European Journal of Operational Research,* 185(3)**,** 1174-1191.

EDRG (2007) The Cost of Highway Limitations and Traffic Delay to Oregon's Economy. Portland, OR.

ERDG (2005) The Cost of Congestion to the Economy of the Portland Region, Economic Research Development Group, December 2005. Boston, MA, accessed June 2008, http://www.portofportland.com/Trade_Trans_Studies.aspx.

ERDG (2007) The Cost of Highway Limitations and Traffic Delay to Oregon's Economy, Economic Research Development Group, March 2007. Boston, MA, accessed October 2008, http://www.portofportland.com/Trade_Trans_Studies_CostHwy_Lmtns.pdf.

FIGLIOZZI, M. A. (2007) Analysis of the efficiency of urban commercial vehicle tours: Data collection, methodology, and policy implications. *Transportation Research Part B,* 41(9)**,** 1014-1032.

FIGLIOZZI, M. A. (2009a) The Impact of Congestion on Commercial Vehicle Tours and Costs. *Transportation Research part E: Logistics and Transportation*, 46(4): p. 496-506.

FIGLIOZZI, M. A. (2009b) An Iterative Route Construction and Improvement Algorithm for the Vehicle Routing Problem with Soft-time Windows. *Transportation Research Part C: New* Technologies, 18(5), p. 668-679.

FIGLIOZZI, M. A. (2009c) A Route Improvement Algorithm for the Vehicle Routing Problem with Time Dependent Travel Times. *Proceeding of the 88th Transportation Research Board Annual Meeting CD rom.* Washington, DC, January 2009, also available at http://web.cecs.pdx.edu/~maf/publications.html.

FIGLIOZZI, M. A. (2010), Vehicle Routing Problem for Emissions Minimization, 2010, *Transportation Research Record* 2197, p.1-7

FLEISCHMANN, B., GIETZ, M. & GNUTZMANN, S. (2004) Time-varying travel times in vehicle routing. *Transportation Science,* 38(2)**,** 160-173.

FREY, H., ROUPHAIL, N. & ZHAI, H. (2008) Link-Based Emission Factors for Heavy-Duty Diesel Trucks Based on Real-World Data. *Transportation Research Record,* 2058(23-332.

GOLOB, T. F. & REGAN, A. C. (2001) Impacts of highway congestion on freight operations: perceptions of trucking industry managers. *Transportation Research Part A: Policy and Practice,* 35(7)**,** 577-599.

HAGHANI, A. & JUNG, S. (2005) A dynamic vehicle routing problem with time-dependent travel times. *Computers & Operations Research,* 32(11)**,** 2959-2986.

HOLGUIN-VERAS, J., WANG, Q., XU, N., OZBAY, K., CETIN, M. & POLIMENI, J. (2006) The impacts of time of day pricing on the behavior of freight carriers in a congested urban area: Implications to road pricing. *Transportation Research Part A-Policy And Practice,* 40(9)**,** 744-766.

ICF (2006) Assessment of Greenhouse Gas Analysis Techniques for Transportation Projects, NCHRP Project 25-25 Task 17, ICF Consulting. Fairfax, VA.

ICHOUA, S., GENDREAU, M. & POTVIN, J. Y. (2003) Vehicle dispatching with time-dependent travel times. *European Journal Of Operational Research,* 144(2)**,** 379-396.

JUNG, S. & HAGHANI, A. (2001) Genetic Algorithm for the Time-Dependent Vehicle Routing Problem. *Transportation Research Record,* 1771(-1)**,** 164-171.

LÉONARDI, J. & BAUMGARTNER, M. (2004) CO_2 efficiency in road freight transportation: Status quo, measures and potential. *Transportation Research Part D,* 9(6)**,** 451-464.

MALANDRAKI, C. (1989) Time dependent vehicle routing problems: Formulations, solution algorithms and computational experiments. Evanston, Illinois., Ph.D. Dissertation, Northwestern University.

MALANDRAKI, C. & DASKIN, M. S. (1992) Time-Dependent Vehicle-Routing Problems - Formulations, Properties And Heuristic Algorithms. *Transportation Science,* 26(3)**,** 185-200.

OECD (2003) *Delivering the Goods 21st Century Challenges to Urban Goods Transport*, OECD Organisation for Economic Co-operation and Development.

PALMER, A. (2008) The development of an integrated routing and carbon dioxide emissions model for goods vehicles. *PhD Thesis Cranfield University November 2007*.

QUAK, H. J. & DE KOSTER, M. B. M. (2007) Exploring retailers' sensitivity to local sustainability policies. *Journal of Operations Management,* 25(6)**,** 1103.

QUAK, H. J. H. & DE KOSTER, M. (2009) Delivering Goods in Urban Areas: How to Deal with Urban Policy Restrictions and the Environment. *Transportation Science,* 43(2)**,** 211-227.

ROPKINS, K., BEEBE, J., LI, H., DAHAM, B., TATE, J., BELL, M. & ANDREWS, G. (2009) Real-World Vehicle Exhaust Emissions Monitoring: Review and Critical Discussion. *Critical Reviews in Environmental Science and Technology,* 39(2)**,** 79-152.

SBIHI, A. & EGLESE, R. W. (2007) Combinatorial optimization and Green Logistics. *4OR: A Quarterly Journal of Operations Research,* 5(2)**,** 99-116.

SOLOMON, M. M. (1987) Algorithms For The Vehicle-Routing And Scheduling Problems With Time Window Constraints. *Operations Research,* 35(2)**,** 254-265.

TANIGUCHI, E., THOMPSON, R. G. & YAMADA, T. (2003) Predicting the effects of city logistics schemes. *Transport Reviews,* 23(4)**,** 489-515.

TRL (1999) Methodology for calculating transport emissions and energy consumption. *Transport Research Laboratory, Crowthorne, United Kingdom.* Edited by A J Hickman, Project Report SE/491/98, Deliverable 22 for the project MEET (Methodologies for estimating air pollutant emissions from transport).

WEISBROD, G., DONALD, V. & TREYZ, G. (2001) Economic Implications of Congestion. NCHRP Report #463. Washington, DC, National Cooperative Highway Research Program, Transportation Research Board.

WHEELER, N. & FIGLIOZZI, M. A. (2009) Multi-Criteria Trucking Freeway Performance Measures in Congested Corridors, 2011 *Transportation Research Record 2224*, p. 82-93.

WOENSEL, T. V., CRETEN, R. & VANDAELE, N. (2001) Managing the environmental externalities of traffic logistics: The issue of emissions. *Production and Operations Management,* 10(2)**,** 207-223.

WOLFE, M., MONSERE, C., KOONCE, P. & BERTINI, R. L. (2007) Improving Arterial Performance Measurement Using Traffic Signal System Data. *Intelligent Transportation Systems Conference, 2007. ITSC 2007. IEEE***,** 113-118.

APPENDIX

Bottleneck Radius Algorithm H_{yr}

Input
$\mathbf{O_n^p}$, $\mathbf{R_n}$, $\mathbf{U_{n+1}^p}$, $\mathbf{L_n}$, $\mathbf{\bar{O}_n}$

START H_{yc}
$\mathbf{R_n^p} \leftarrow \emptyset$
For $m \in \mathbb{N} = 1$ to n
$\qquad \mathbf{R^p} \leftarrow \emptyset$
$\qquad R \leftarrow R_m$
$\qquad$ **For** $k \in \mathbb{N} = 1$ **To** p
$\qquad\qquad$ **If** $O_{km} \geq \bar{O}_m$ **Then**
$\qquad\qquad\qquad R \leftarrow R + \left|U_{k,m+1} - U_{km}\right|\left(t_{\bar{k}} - t_{\underline{k}}\right)L_m$
$\qquad\qquad$ **Else**
$\qquad\qquad\qquad$ **If** $O_{km} < \bar{O}_m$ **And** $R > \bar{R}_m$ **Then**
$\qquad\qquad\qquad\qquad R \leftarrow R - \left|U_{k,m+1} - U_{km}\right|\left(t_{\bar{k}} - t_{\underline{k}}\right)L_m$
$\qquad\qquad\qquad$ **Else**
$\qquad\qquad\qquad\qquad R \leftarrow R_m$
$\qquad\qquad\qquad$ **End If**
$\qquad\qquad$ **End If**
$\qquad\qquad \mathbf{R^p} \cup R$
$\qquad$ **Next** k
$\qquad \mathbf{R_n^p} \cup \mathbf{R^p}$
Next m
Output: $\mathbf{R_n^p} = [R_{km}]_{p \times n}$

51

Arrival time algorithm H_{yf}

Input
$\mathbf{R_n^p}, \mathbf{T_p}, \ a_i, b_i, e_i, \ g_i, v_i, v_j, u_{ij}$
START H_{yf}
If $a_i < e_i$ **Then**
       $b_i \leftarrow e_i + g_i$
Else
       $b_i \leftarrow a_i + g_i$
End If
$D_{ij} \leftarrow f(x_i, x_j, y_i, y_j)$
Find $k, t_{\underline{k}} \leq b_i \leq t_{\bar{k}}$
       $k \leftarrow k$
$\mathbf{S_n} \leftarrow \emptyset$
For $m = 1 \in \mathbb{N}$ **To** n
       $D_{jm} \leftarrow f(x_j, x_m, y_j, y_m)$
       $D_{im} \leftarrow f(x_i, x_m, y_i, y_m)$

$$r \leftarrow \sqrt{\left(\frac{d}{d_{ij}}D_{ij}\right)^2 + D_{jm}^2 - \frac{d}{d_{ij}}\left(D_{ij}^2 + D_{jm}^2 - D_{im}^2\right)}$$

       If $r \leq R_{km}$ **Then**
$$s_m \leftarrow u_{ij}\frac{v_{km}}{w_m}$$
       Else
           $s_m \leftarrow u_{ij}$
       End If
       $\mathbf{S_n} \leftarrow \mathbf{S_n} \cup \{s_m\}$
Next m
$s \leftarrow \min[\mathbf{S_n}]$
$d \leftarrow d_{ij}$
$a_j \leftarrow b_i + \frac{d}{s}$
$t \leftarrow b_i$
While $a_j > t_{\bar{k}}$ **Do**
       $d \leftarrow d - (t_{\bar{k}} - t)s$
       $t \leftarrow t_{\bar{k}}$
       $k \leftarrow k + 1$
       $\mathbf{S_n} \leftarrow \emptyset$
       For $m \in \mathbb{N} = 1$ **To** n
           $D_{jm} \leftarrow f(x_j, x_m, y_j, y_m)$
           $D_{im} \leftarrow f(x_i, x_m, y_i, y_m)$

$$r \leftarrow \sqrt{\left(\frac{d}{d_{ij}}D_{ij}\right)^2 + D_{jm}^2 - \frac{d}{d_{ij}}\left(D_{ij}^2 + D_{jm}^2 - D_{im}^2\right)}$$

           If $r \leq R_{km}$ **Then**

$$s_m \leftarrow u_{ij}\frac{v_{km}}{w_m}$$

Else

$$s_m \leftarrow u_{ij}$$

End If

$$\mathbf{S_n} \leftarrow \mathbf{S_n} \cup \{s_m\}$$

Next m

$$s \leftarrow \min[\mathbf{S_n}]$$

$$a_j \leftarrow t + \frac{d}{s}$$

End While

Output: a_j

Departure time algorithm H_{yb}

Input
$\mathbf{R_n^p}, \mathbf{T_p}, \mathbf{v_n^p}\; a_j,\, e_i,\, g_i,\, v_i\,, v_j,\, u_{ij}$

START
$D_{ij} \leftarrow f(x_i, x_j, y_i, y_j)$
Find $k, t_{\underline{k}} \le a_j \le t_{\bar{k}}$
$\qquad k \leftarrow k$
$\mathbf{S_n} \leftarrow \emptyset$
For $m = 1 \in \mathbb{N}$ **To** n
$\qquad D_{jm} \leftarrow f(x_j, x_m, y_j, y_m)$
$\qquad D_{im} \leftarrow f(x_i, x_m, y_i, y_m)$
$\qquad r \leftarrow \sqrt{\left(\frac{d}{d_{ij}} D_{ij}\right)^2 + D_{im}^2 - \frac{d}{d_{ij}}\left(D_{ij}^2 + D_{im}^2 - D_{jm}^2\right)}$
$\qquad$ **If** $r \le R_{km}$ **Then**
$\qquad\qquad s_m \leftarrow u_{ij} \dfrac{v_{km}}{w_m}$
$\qquad$ **Else**
$\qquad\qquad s_m \leftarrow u_{ij}$
$\qquad$ **End If**
$\qquad \mathbf{S_n} \leftarrow \mathbf{S_n} \cup \{s_m\}$
Next m
$s \leftarrow \min[\mathbf{S_n}]$
$d \leftarrow d_{ij}$
$t \leftarrow a_j$
$d_k \leftarrow (t - t_{\underline{k}})s$
While $d_k < d$ **And** $k > 0$ **And** $t_{\bar{k}} > e_i$ **Do**
$\qquad d \leftarrow d - d_k$
$\qquad \mathbf{S_n} \leftarrow \emptyset$
$\qquad$ **For** $m \in \mathbb{N} = 1$ **To** n
$\qquad\qquad D_{jm} \leftarrow f(x_j, x_m, y_j, y_m)$
$\qquad\qquad D_{im} \leftarrow f(x_i, x_m, y_i, y_m)$
$\qquad\qquad r \leftarrow \sqrt{\left(\frac{d}{d_{ij}} D_{ij}\right)^2 + D_{jm}^2 - \frac{d}{d_{ij}}\left(D_{ij}^2 + D_{jm}^2 - D_{im}^2\right)}$
$\qquad\qquad$ **If** $r \le R_{km}$ **Then**
$\qquad\qquad\qquad s_m \leftarrow u_{ij} \dfrac{v_{km}}{w_m}$
$\qquad\qquad$ **Else**
$\qquad\qquad\qquad s_m \leftarrow u_{ij}$
$\qquad\qquad$ **End If**
$\qquad\qquad \mathbf{S_n} \leftarrow \mathbf{S_n} \cup \{s_m\}$

Next m

$s \leftarrow \min[\mathbf{S_n}]$

$t \leftarrow t_{\underline{k}}$

$b_i \leftarrow t - \dfrac{d}{s}$

$k \leftarrow k - 1$

$d_k \leftarrow \left(t - t_{\underline{k}}\right)s$

End While

If $d_k \geq d$ **Then**

$\qquad b_i \leftarrow t_{\bar{k}} - \dfrac{d}{s}$

Else

$\qquad b_i \leftarrow -\infty$

Output: b_i

OTREC

**OREGON TRANSPORTATION RESEARCH
AND EDUCATION CONSORTIUM**

P.O. Box 751
Portland, OR 97207

OTREC is dedicated to
stimulating and conducting
collaborative multi-disciplinary
research on multi-modal surface
transportation issues, educating
a diverse array of current
practitioners and future leaders
in the transportation field, and
encouraging implementation of
relevant research results.